

Protein–Nanoparticle Interactions: Opportunities and Challenges

Morteza Mahmoudi,^{*,†,‡} Iseult Lynch,[§] Mohammad Reza Ejtehadi,^{||} Marco P. Monopoli,[§] Francesca Baldelli Bombelli,[°] and Sophie Laurent[⊥]

[†]National Cell Bank, Pasteur Institute of Iran, Tehran, Iran

[‡]Nanotechnology Research Center, Faculty of Pharmacy, Tehran University of Medical Sciences, Tehran, Iran

[§]School of Chemistry and Chemical Biology & Conway Institute for Biomolecular and Biomedical Research, University College Dublin, Belfield, Dublin 4, Ireland

^{||}Department of Physics, Sharif University of Technology, Tehran, Iran

[°]School of Pharmacy, UEA, Norwich Research Park, Norwich, U.K.

[⊥]Department of General, Organic, and Biomedical Chemistry, NMR and Molecular Imaging Laboratory, University of Mons, Avenue Maistriau 19, B-7000 Mons, Belgium

CONTENTS

1. Introduction	5610	5.2.2. Isothermal Titration Calorimetry	5622
2. Formation of the Protein Corona	5611	5.2.3. ζ Potential	5623
2.1. Thermodynamic and Kinetic Aspects of the NP–Protein Corona	5613	5.2.4. Differential Centrifugal Sedimentation	5623
3. Effects of NPs on Corona Composition	5614	5.3. X-ray Crystallography	5623
3.1. Effects of NP Composition	5615	5.4. Chromatography	5623
3.2. Effect of NP Size	5615	5.4.1. Electrophoresis	5624
3.3. Effect of NP Shape	5616	5.4.2. Mass Spectrometry	5624
3.4. Effect of NP Crystallinity	5616	5.4.3. Surface Plasmon Resonance	5626
3.5. Effect of NP Surface Area	5616	5.4.4. Quartz Crystal Microbalance	5627
3.6. Effect of Surface Defects	5616	5.5. Advantages and Limitations of the Available Methods	5627
3.7. Effects of NP Surface Properties	5616	5.6. Request for Possible New Methods	5627
3.7.1. Effect of Charge	5616	6. Simulation of NP–Protein Interactions	5627
3.7.2. Effects of Smoothness/Roughness	5616	6.1. Simulation Results for NP–Protein Interactions	5630
3.7.3. Electron Transfer Capability	5616	6.2. NP Self-Assembly	5631
3.7.4. Effects of Hydrophobicity/Hydrophilicity	5616	6.3. NPs in Larger Biological Systems	5631
3.7.5. Protein/NP Ratio	5617	7. Outcome of Protein–NP Interactions	5631
3.7.6. Effect of Functional Groups and Targeting Moieties	5617	8. What Is Next?	5631
4. Conformational Changes of Proteins upon Binding to NPs	5617	9. Conclusions	5632
4.1. Reversible Conformational Changes	5618	Author Information	5632
4.2. Irreversible Conformational Changes	5619	Biographies	5632
5. Analytical Methods for Corona Evaluation	5620	Acknowledgment	5634
5.1. Spectroscopy Methods	5621	References	5634
5.1.1. UV/Vis	5621		
5.1.2. Fluorescence	5621		
5.1.3. Fourier Transform Infrared and Raman Spectroscopy	5621		
5.1.4. Circular Dichroism	5621		
5.1.5. Nuclear Magnetic Resonance	5622		
5.2. Other Methods	5622		
5.2.1. Dynamic Light Scattering	5622		

1. INTRODUCTION

In recent years, the fabrication of nanomaterials and exploration of their properties have attracted the attention of all branches of science, such as physics, chemistry, biology, and engineering.^{1–4} Interest in nanoparticles (NPs) arises from the fact that the mechanical, chemical, electrical, optical, magnetic, electro-optical, and magneto-optical properties can be completely different from those of their bulk counterparts, and these

Received: December 19, 2010

Published: June 21, 2011

differences are dependent on the particle size.^{5–7} From a biological and medical applications viewpoint, the primary interest in nanoparticles stems from the fact that they are small enough to interact with cellular machinery and potentially to reach previously inaccessible targets, such as the brain.^{8,9} There are numerous areas where nanoparticulate systems are of significant scientific and technological interest, specifically for biomedicine leading to concern for the design of safe nanobiomaterials. Nanoparticles also find large scale use in information technology applications and in several industry areas with potential for unintentional exposure to the environment or living matter during processing or at the end of a nanotechnology-containing product's life cycle. In fact, the large use of nanomaterials in industrial processes has promoted the study of nanotoxicology and highlighted the need for safety assessment research to be performed in parallel to development of applications.^{10,11}

It is now well-recognized that the surfaces of biomaterials (e.g., implants and medical devices) are immediately covered by biomolecules (e.g., proteins, natural organic materials, detergents, and enzymes) when they come in contact with a biological medium.^{12–18} The absorption of biomolecules to such surfaces confers a new “biological identity” in the biological milieu, which determines the subsequent cellular/tissue responses.^{19,20} Due to their extremely high surface to volume ratio, NPs have a very active surface chemistry in comparison to bulk biomaterials; hence, in biological applications they tend to reduce their large surface energy by interaction with the medium components in which they are dispersed.^{21,22} Thus, the dispersion of NPs in a biological medium results in their surfaces (as with bulk materials) being covered by a complex layer of biomolecules.

Interestingly, the interaction between nanomaterials and environmental biomolecules results in the formation of a biological corona on the NP's surface that is quite dramatically different from that adsorbed on a flat surface of the same bulk material. In the same experimental conditions the adsorbed protein layer that forms on flat surfaces of the same bulk material, in both protein composition and organization of the associated proteins, with quite different biological consequences.²⁰ Therefore, what a biological entity, such as cells, tissues, and organs, actually “sees” when interacting with NPs is completely different from the original pristine surface of the NPs. This new biological identity of the NP is achieved by creation of a new interface between the NPs and the biological medium, the so-called “bio-nano interface”.^{12,23–26}

Formation of the corona is a dynamic, competitive process. The proteins present in a biofluid compete for the NP surface to form a bio-nano interface, the so-called “protein corona”.^{13,20,27,28} This protein corona evolves rapidly from that which forms upon initial introduction of the NPs into the biological fluid, due to exchange of low-affinity high-abundance proteins that bind immediately by lower abundance proteins with a higher affinity for the NP surface, as well as ongoing exchange between the NP-adsorbed proteins and free proteins in the medium. It is notable that this corona constitutes the primary contact to the cells,^{12,13,23,24} including interaction with cellular receptors during uptake.^{13,29–33} Although there are several thousand proteins in human biological fluids competing to bind to the NP's surface, the protein corona is usually enriched with about 10–50 proteins that have the highest affinity for the surface. However, the formation of the corona is a complex dynamic process, and a deep understanding of both the thermodynamics and kinetics of the protein corona evolution and its subsequent biological impacts requires, development of new advanced tools to investigate the bio-nano interface, giving special

attention to screening of the outer amino acid sequences (epitopes) that are in contact with living systems. In this regard, very few reports are available,^{34–38} and an additional complication is that single protein–NP interactions are not helpful to predict the formation of the corona for which cooperative effects are expected to provide the driving force.

The potentially high concentration of proteins adsorbed on the surface of NPs, together with their low dimensionality, can enhance the probability of partial protein unfolding. This can potentially lead to faster protein association with the formation of new protein clusters, which may be recognized as harmful products (and can potentially contribute to the progress of diseases such as amyloidosis^{39–41}) or could introduce new biological interactions, as a result of new protein surface presentations (new epitopes) at the bio/nano interface.^{42–44}

The biological responses to NPs are highly affected by the main forces at the bio-nano interface (e.g., hydrodynamic, electrodynamic, and electrostatic or steric forces and solvent and polymer bridging) and also by the intrinsic characteristics of the NPs (e.g., size, shape, charge, coatings, surface modifications with targeting ligands, crystallinity, electronic states, surface wrapping in the biological medium, hydrophobicity, and wettability), which drive the formation of the protein corona. Therefore, a better understanding of the NP–protein complex is essential to the development of functional and safe NPs.²³

The importance of the physicochemical characteristics of NPs on the nature of the corona formed is discussed in detail, followed by comprehensive descriptions of the currently available evaluation methods for assessing the protein corona. The limitations of available methods (e.g., spectroscopy methods (UV/vis, Raman, fluorescence, mass spectrometry, nuclear magnetic resonance, etc.), dynamic light scattering, circular dichroism, differential centrifugal sedimentation, scanning and transmission electron microscopies, X-ray crystallography, chromatography, etc.) for assessing NP–protein (biomolecule) complexes *in situ* are probed in detail, followed by a discussion of the possibilities for enhancing the current methods and a request for new techniques. Furthermore, the advantages and disadvantages of the protein–NP interaction phenomena are explored and discussed in terms of the corresponding biological impacts. This review also presents a broad overview of both *in vitro* and *in vivo* data on the role of protein–NP interactions in determining NP fate and behavior. Readers will obtain a deep understanding of the effect of the NP physicochemical properties (i.e., size and size distribution, shape, composition, surface chemistry, coatings, etc.) on the final structure, composition and function of NP–protein complexes present in biological fluids and on their possible impact on the NPs fate and behavior *in vivo* (e.g., conformation and function) they preferentially adsorb to their surfaces, with the advantages and disadvantages of the outcome for the various proteins following their interaction with NPs. In addition, the reader will discover the further steps required to fully understand the role of protein–NP interactions in determining NP fate and behavior.

2. FORMATION OF THE PROTEIN CORONA

It is now well-recognized that the ability to generate ever-smaller NPs, together with increasing control of their physicochemical properties, has been driven by the development of an increasing range of potential applications of nanotechnology.⁴⁵ By reducing the size of the NPs, the number of atoms located at the surface is considerably increased, leading to a significant enhancement of their chemical reactivity. NPs designed for use in

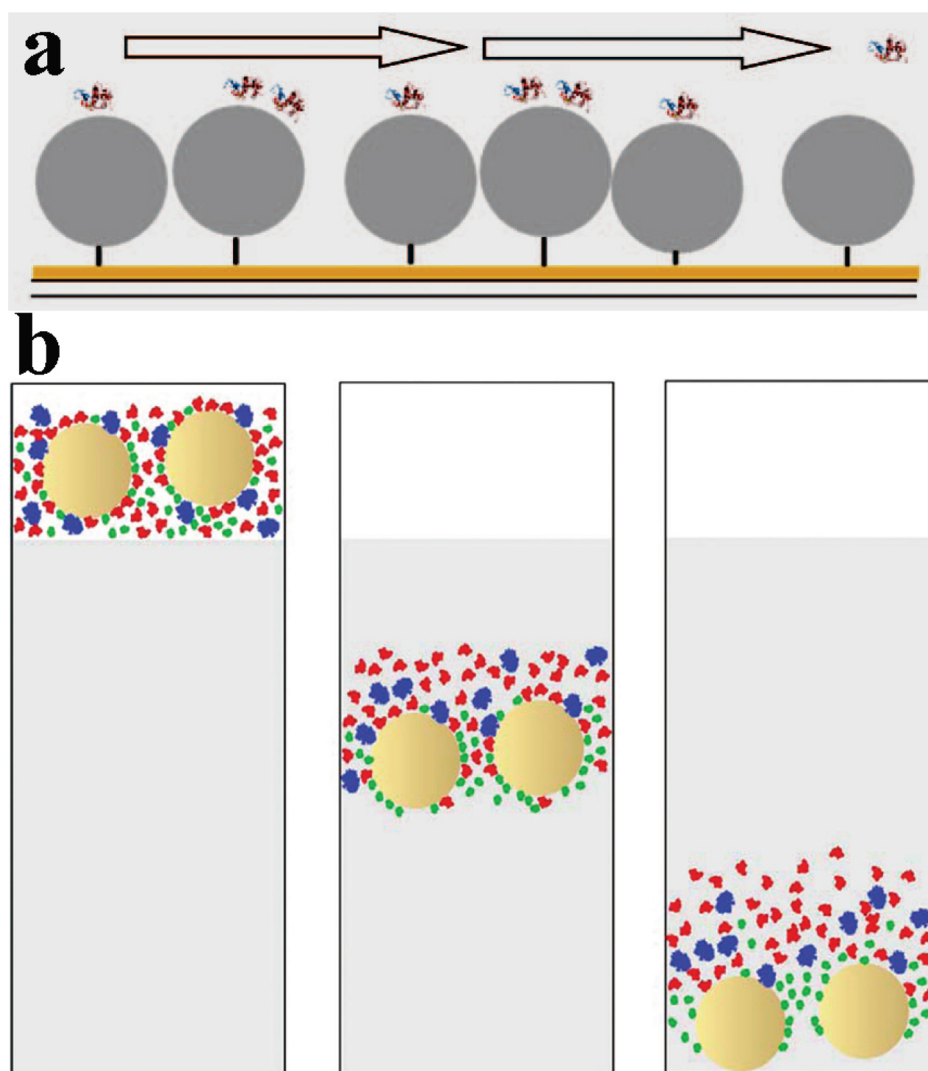


Figure 1. (a) Schematic representation of a gold surface with thiol-tethered particles and associated proteins over which buffer is flown to remove the unbound proteins and to determine the dissociation kinetics. (b) Gel filtration of NP–protein mixture. NPs (beige) are applied to an SEC column in a protein mixture, symbolized by a large blue protein of low abundance and medium off rate, a red protein of high abundance and higher off rate, and a green protein of high abundance and low off rate. In the eluate, the green protein is preferentially enriched on the particles, whereas the faster dissociating proteins elute later. Reprinted with permission from ref 12. Copyright 2007 National Academy of Sciences.

biomedical applications, more specifically for targeted drug delivery and imaging purposes, will likely require intravenous injection.^{46,47} Upon entrance of the NPs into the biological environment, such as into the bloodstream (plasma), their surfaces will be rapidly covered by selective sets of blood plasma proteins, forming the so-called “protein corona”.^{12,24,25,30,48,49} For other routes of exposure, before coming into contact with the plasma proteins, the NPs have to pass through the physiological barriers of the body (i.e., skin, gastrointestinal tract, lung), picking up biomolecules as they are transported.⁵⁰ The protein-coated particles may transmit a number of biological effects, due to variation in the nature of the adsorbed proteins or variations in adsorbed protein conformations (in either a reversible or irreversible manner), exposure of new epitopes, and perturbation of protein function, together with potential avidity effects arising from the close spatial repetition of the same protein.¹²

It has been shown that the protein corona is composed of an inner layer of selected proteins with a lifetime of several hours in slow exchange with the environment (hard corona) and an outer layer of

weakly bound proteins which are characterized by a faster exchange rate with the free proteins (the soft corona).⁴⁹ Due to the long lifetime of the hard protein corona, it is now believed that the hard corona rather than the pristine NP surface interacts with cellular receptors and defines the fate of NPs in a biological environment. Therefore, identification of the adsorbed proteins and their lifetimes and conformations at the NP surface is considered a vital research question with deep implications for the design of safe nanomedicines and nanoenabled consumer products. By understanding NP–protein interactions, one can potentially define and predict NP–cell interactions and elucidate the safety considerations for biomedical applications, resulting in NPs that are “safe by design”.

Several parameters can influence the characteristics of an NP–protein corona, including the physicochemical properties of the specific NPs and the distinctiveness of the adsorbed proteins.^{23,35}

It is notable that the biological impact of protein-coated NPs is mainly related to the proteins with the highest affinity (i.e., the hard corona) and their specificity and suitable orientation for a

particular receptor response, rather than to effects from low-affinity high-abundance proteins, which might bind initially but are quickly replaced by lower abundance and higher affinity proteins. Thus, evaluation of protein lifetimes on the surface of NPs is a critical matter for the assessment of NP biological response, as proteins that exchange rapidly with respect to the time scale of the cellular processes will not be decisive, while more strongly bound proteins (hard corona) will likely mediate the NP interactions with living matter.⁴⁸ Hence, a deep understanding of the structure and affinity of the adsorbed proteins on the surface of NPs is needed, and at present, the proteins must be isolated from the surface of the NPs to achieve this characterization.

Isolation of the nanoparticle–protein complex process is a complicated task and not easy to achieve. For instance, the common method is centrifugation and washing of NPs, which allows the removal of unbound proteins and those with low binding energy.^{51–54} More recently, it was shown that, using differential sedimentation centrifugation (DCS), essentially identical results for the protein corona *in situ* in plasma and following isolation by centrifugation and washing were obtained, indicating how robust the “hard corona” is and confirming that approaches where the protein–NP complexes are removed from unbound proteins for physicochemical characterization are appropriate and provide meaningful information on the *in situ* NP–protein complex.⁴⁸ There is great interest to develop new methods for investigation on of both soft and hard coronas in order to shed light on the complex mechanism of competitive binding among the plasma proteins when the system is under kinetic or thermodynamic control.^{12,35} In addition, the developed methods should have the capability to separate proteins with various affinities, without any disruption of the protein–NP complexes, as well as avoiding the creation of new binding opportunities. Cedervall et al.¹² proposed size-exclusion chromatography (SEC), isothermal titration calorimetry (ITC), and surface plasmon resonance (SPR) as suitable methods to determine various aspects of NP–protein interactions, including the affinities of various proteins for the NP surface. Four different tailored *N*-isopropylacrylamide (NIPAM)/*N*-*tert*-butylacrylamide (BAM) copolymer NPs of increasing surface hydrophobicity were employed, and it has been shown that ITC is suitable for probing the stoichiometry of the proteins bound to the surface of NPs. However, limitations of this method are that, to provide detailed thermodynamic and stoichiometric information, an enthalpic change must result from the interaction between the NP and the protein and that single-protein–NP studies are needed to provide quantitative information,²⁵ as whole plasma studies resulted in data averaged over all proteins. Moreover, the protein exchange rates and affinities for the NP surface were determined by employing SPR technology with the NPs thiol-linked to a gold chip and through size-exclusion chromatography of protein–NP mixtures (see Figure 1a). The results from this early study on NP–plasma interactions confirmed that SEC is potentially less perturbing of protein–particle complexes than centrifugation. In addition, SEC–gel filtration was employed to define both the characteristics of the proteins on the surface of NPs with the exchange rates with free plasma proteins (see Figure 1b). Subsequent systematic studies have shown that a robust protocol with careful centrifugation and washing steps can yield similar highly reproducible coronas.^{12,21,24} The isolation yield of SEC–gel filtration can be enhanced by optimizing the column dimensions and relative concentrations of both proteins and NPs followed by proteomics/mass spectrometry methods for identification of the bound proteins.

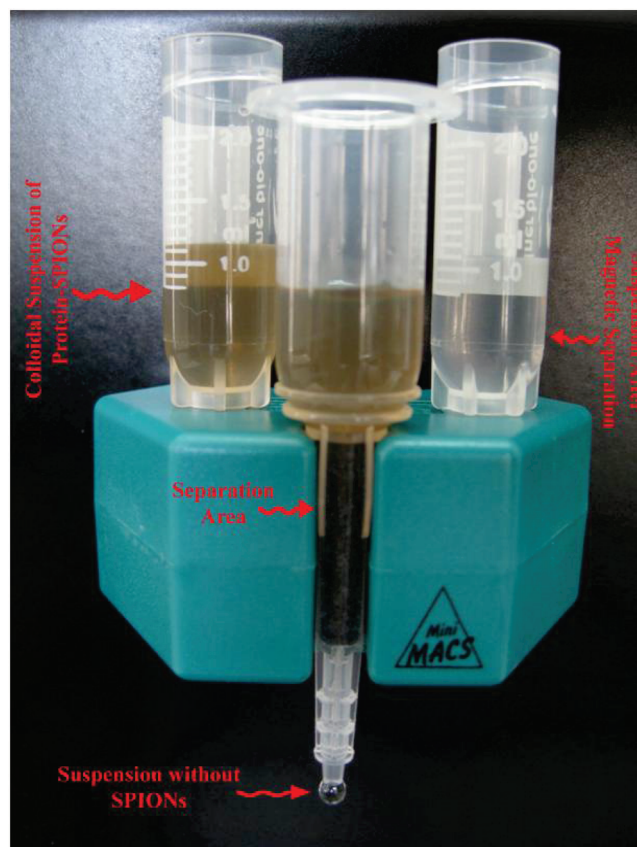


Figure 2. Experimental setup for determination of the proteins bound to magnetic NPs (SPIONs). The MACS columns are composed of a spherical steel matrix; by inserting a column in a MACS separator, a high-gradient magnetic field is induced within the column which retains the SPIONs. Reprinted with permission from ref 35. Copyright 2011 Royal Society of Chemistry.

Further advances in both quantitative and qualitative analyses (e.g., the conformation and geometry of proteins) of the soft and hard coronas are emerging. Mahmoudi et al.³⁵ introduced a method for characterization of protein coronas surrounding magnetic NPs. It is notable that superparamagnetic iron oxide NPs (SPIONs) have been used, due to their special magnetic properties together with their very good biocompatibility, which made them preferential to other magnetic NPs.^{13,27,28,30,35,46,49,55–60} In this approach, after the interaction of the magnetic NPs with proteins for the desired time, the protein-associated magnetic NPs were run through a strong magnetic field using magnetic-activated cell sorting (MACS), leading to fixing of the magnetic NPs in the magnetic column (see Figure 2). Subsequently, the flow-through fraction which contains the free (non-NP-bound) proteins was collected, and the trapped NPs were washed with various molarities of protein washing solutions (e.g., various molarities of KCl) to define the binding affinity of the proteins to the various SPIONs.

2.1. Thermodynamic and Kinetic Aspects of the NP–Protein Corona

Defining both the thermodynamics and kinetics of the formation of NP–protein coronas is considered of crucial importance for determination of the corona composition and subsequent environmental or biological impacts. For instance, the kinetics of reactions occurring at the bio-nano interface, including competitive binding processes and concurrent exchange with free

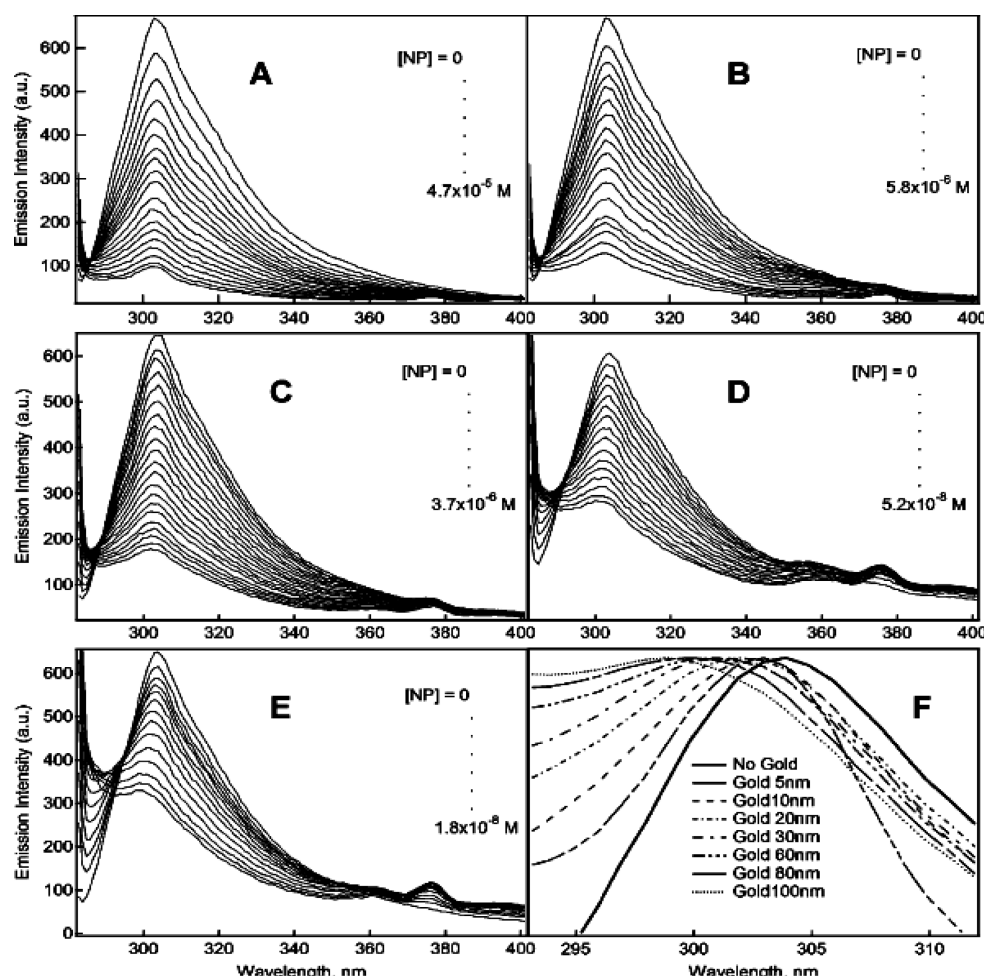


Figure 3. Fluorescence quenching of histone (H3) by gold NPs of (A) 5 nm, (B) 10 nm, (C) 20 nm, (D) 60 nm, and (E) 100 nm and (F) expanded and normalized emission spectra of histone in the absence or presence of gold NPs showing a shift of the emission peak. The normalization is defined so that the emission peak intensity is divided by the maximum of the fluorescence emission spectrum intensity such that the normalized peak intensity equals 1. The protein concentration was fixed at 0.01 mg/mL, and the NP concentration was varied over the range (A) from 0 to 4.7×10^{-6} M (5 nm), (B) from 0 to 5.8×10^{-6} M (10 nm), (C) from 0 to 3.7×10^{-6} M (20 nm), (D) from 0 to 5.2×10^{-8} M (60 nm), and (E) from 0 to 1.8×10^{-8} M (100 nm). Reprinted from ref 34. Copyright 2010 American Chemical Society.

proteins in the media, have an important role in determining the interactions of NPs not only with biological surfaces but also with cellular receptors.²³ The stoichiometry, affinity, and enthalpy of protein–NP interactions can be determined using ITC.^{12,25}

The kinetics of protein adsorption on the surface of NPs is recognized to be critical for the prediction of the fate of NPs in biological fluids. A complete understanding of the mechanism of formation and exchange of the soft corona is hard to achieve due to the interplay of various phenomena; however, there is considerable knowledge regarding competitive protein binding to surfaces from the medical device community.^{12,13,27} The Vroman effect describes how proteins that adsorb first to the surface are later replaced by other proteins with higher affinity for the surface. The Vroman effect is dependent on the concentration of the proteins relative to the available surface area together with their diffusion coefficients, which can affect the affinity of proteins for the surface, and applies to macroscale surfaces.^{45,61} However, the high surface curvature and the very large surface area of NPs mean that different behaviors emerge with NPs,¹² and indeed, the interplay of the different factors can lead to different consequences for different NPs. For instance, due to its

high affinity, fibrinogen is rapidly depleted near surfaces of polystyrene NPs with various functional groups (e.g., COOH and CH₃), hence allowing lower affinity proteins with higher abundance (e.g., albumin) to adsorb provisionally, to be subsequently replaced by fibrinogen.⁴⁵ The effect of the protein concentration to NP surface area ratio also plays a role here, with a deep decrease in the affinity of fibrinogen for sulfonated polystyrene nanoparticles with increasing plasma concentration (at constant particle surface area).²²

3. EFFECTS OF NPs ON CORONA COMPOSITION

There are several different components that affect the complex interactions at the bio-nano interface, such as the physiochemical properties of the NPs themselves, the composition of the biological fluid, and the resulting protein corona with possible reversible/irreversible conformational changes of the proteins after interaction with NPs.²³ In this section, the most important physical-chemical characteristics of the NPs influencing the nature of NP–protein coronas are discussed in detail.

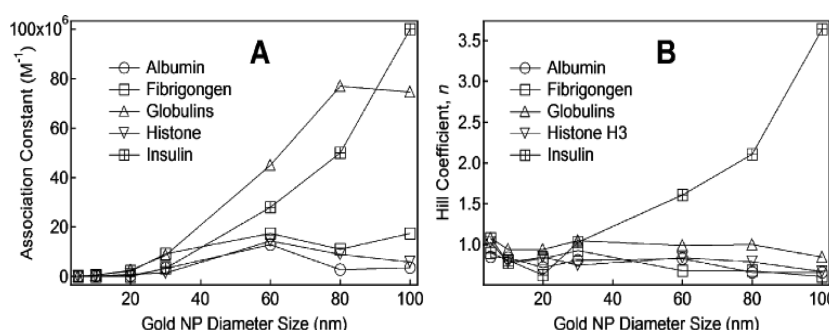


Figure 4. Effect of the size of gold NPs on protein association: (A) effect of NP size on the binding association constant of the gold NP–protein complex, (B) effect of NP size on the Hill coefficient, n , a quantitative measure of the cooperativity of mutual NP–protein binding. Reprinted from ref 34. Copyright 2010 American Chemical Society.

3.1. Effects of NP Composition

The affinities and amounts of proteins adsorbed on the surfaces of NPs are highly dependent on the nanomaterial composition and its surface chemistry.^{52,62,63} For instance, the corona that formed around copolymer NPs was shown to be sensitive to the surface hydrophobicity and the availability of -CH₃ groups (reminiscent of fatty acid chains) present at the NP surface, with apolipoproteins having highest affinity for the most hydrophobic NPs.^{12, 24} copolymer particles, cerium oxide particles, quantum dots, and carbon nanotubes, are all found to reduce the lag (nucleation of fibrils) phase of human β_2 -microglobulin, and the observed reduction was highly dependent on the amount and nature of the particle surface.⁴⁴

3.2. Effect of NP Size

The curvature of the NP surface, which is dependent on the size of the NPs, can have a significant influence on the adsorption of biomolecules, which undergo different conformational changes from their native structure with respect to those observed for the protein adsorbed onto flat surfaces of the same material.^{20,26,48} Gold NPs of various sizes (i.e., 5, 10, 20, 30, 60, 80, and 100 nm) were incubated sequentially with common blood proteins, including albumin, fibrinogen, γ -globulin, histone, and insulin.³⁴ According to the results, the gold NPs had significant interaction with each of the proteins; the binding constant and the degree of cooperativity of protein–NP binding (i.e., the Hill constant, n), depended on the NP size. It has also been confirmed by fluorescence F3 443 quenching of histone by gold NPs that the thickness of the protein corona gradually increased with increasing size of the NPs. Figure 3 shows the photoluminescence (PL) quenching patterns for gold NPs of various sizes and concentrations treated with histone. According to Figure 3, a progressive decrease in the emission maximum intensity has been observed with decreasing NP size, where the quenching effect is related to direct interaction of the gold NPs with chromophore residues of the proteins having an interaction radius less than 10 nm.⁶⁴ The change in the maximum of the fluorescence emission spectrum arises from conformational changes of the different proteins upon binding to the gold NPs.^{65–68}

Determination of the binding association constant, k , for all protein–NP pairs should give an idea of the exchange rates of the proteins (about 3700) in blood plasma, but would be very time consuming, and would not account for competitive effects.³⁴ The k values for the binding of the plasma proteins to gold NPs, with various sizes and coatings, were probed by several

groups.^{25,34,67,69,70} For instance, the k values for the binding of chymotrypsin to amino acid functionalized gold NPs and bovine serum albumin to citrate-coated gold NPs are in the range of 10^4 to 10^7 (mol/L)^{−1}.^{67,69} In addition, the k values were tracked for the binding of common blood proteins to gold NPs with a size range between 5 and 100 nm.³⁴ According to the results which are presented in Figure 4, the k values increased gradually with increasing NP size between 5 and 60 nm. In contrast, the k values showed an irregular trend for gold NPs in the size range 60–100 nm; the authors claimed that the conformational state of the adsorbed proteins was responsible for the irregular changes with the larger NP sizes.³⁴ However, other reports confirmed the regular enhancement in k constants by increasing the size of gold NPs, for example, the binding of herceptin-coated gold NPs (size range of 2–70 nm) with ErbB2 receptor or the binding of citrate-functionalized gold NPs (size range of 2–20 nm) with polyfluorenes.^{25,70} In addition to the binding association constant, the Hill coefficient, n , is also a frequently utilized measure of binding cooperativity. The Hill coefficient is also related to the size of the NPs (see Figure 4A). Anticooperative binding was defined for human serum albumin (HSA), fibrinogen, histone, and γ -globulin proteins, and the results indicated within the frame of the Hill model that the association energy per NP gradually decreases with further protein adsorption ($n < 1$); however, the opposite trend was detected for insulin.³⁴ These results highlight two of the challenges of single-protein–NP studies, that quite different results can be obtained depending on the specific protein–NP pair, meaning that every single-protein–particle combination would need to be determined using this approach, and that even should this be done, the constants determined in this manner do not account for competitive or cooperative binding effects whereby the presence of one protein at the NP surface may impede or enhance the binding of another protein to the NP surface.

Cedervall et al.¹² used NPs with various hydrophobicities and probed the protein adsorption on their surfaces. According to their results, there was a distinct difference in the degree of protein surface coverage of the NPs depending on their size, with a larger degree of protein coverage on the larger particles. By decreasing the NP size from 200 to 70 nm, a curvature-induced suppression of the protein adsorption was observed. Klein²¹ claimed that the curvature of smaller NPs may entirely suppress the adsorption of certain proteins, especially for larger or less conformationally flexible proteins; hence, both the NP size and surface composition (e.g., hydrophobicity) of NPs are very important parameters in defining the composition of the formed protein corona.

3.3. Effect of NP Shape

The shape of NP has a great impact not only on its physicochemical characteristics but also on the way that proteins adsorb onto its surface and consequently on the way that cells interact with it. For instance, the shape of gold NPs has a great impact on their interactions with cell layers; more specifically, a peak in cell association for 50 nm spherical gold NPs will be decreased by changing the shape of the NPs to the rod geometry.⁷¹

3.4. Effect of NP Crystallinity

Mahmoudi et al.⁵⁹ showed that a high amount of poly(vinyl alcohol) (PVA) as a coating, usually with a polymer/iron mass ratio greater than 3, reduces the crystallinity of SPIONs and affects the cytotoxicity profile of the obtained materials due to the effect of the crystallinity on the protein adsorption profile on the particle surfaces.²³

3.5. Effect of NP Surface Area

The particle agglomeration behavior can be different for varying particle/protein ratios.⁷² Thus, the particle surface might not be independent of the protein concentration used, and the determination of the protein affinity might be hindered by this. It has also been observed that, for some NPs, the protein concentration to NP surface area ratio has quite dramatic effects on the nature of the adsorbed protein corona. The patterns of binding observed at *in vitro* protein concentrations (3–10% proteins) were very different from those observed at *in vivo* (55–80% proteins) concentrations for sulfonated polystyrene NPs.²²

3.6. Effect of Surface Defects

Năreojă et al.⁷³ investigated the possible effects of well surface defects, well edges, and denaturation of capture antibodies on the specific binding activity of antibodies. Their first aim was to find out if surface defects can be attributed as an origin of nonspecific binding of the bioconjugated nanoparticle label on the capture surface. Therefore, microtiter well surfaces and their patterns were studied with scanning probe microscopy (atomic force microscopy, AFM) and fluorescence microscopy. The second line of approach was to determine to what extent denaturing of surface-bound and soluble antibodies caused unwanted nonspecific binding and to study if the nonspecific binding of bioconjugated nanoparticles having a large surface area compared to soluble label antibodies was connected to the specific binding activity of an antibody.

The same authors have previously studied the effect of the bioconjugated nanoparticle size and fragmented antibodies on nonspecific binding. Neither assay component showed a significant effect on increasing nonspecific binding.⁷⁴ The same conclusion can be drawn from this study: microtiter plate surface defects and denaturation of capture protein did not increase the nonspecific signal in a sandwich immunoassay utilizing bioconjugated nanoparticle labels.⁷⁴

3.7. Effects of NP Surface Properties

3.7.1. Effect of Charge The surface charge of NPs is very important for defining the composition of the formed protein corona and also has an impact on their subsequent biodistribution. For instance, some positive NPs are rapidly identified by opsonins, leading to the removal of the particles by the reticuloendothelial system (RES) and mononuclear phagocytic systems, with their final destination being the liver and spleen, causing a significant decrease in the application yield of these NPs.^{13,27,28,75} Many NPs are stabilized in physiological conditions by functionalization with negatively charged groups (carboxylated, sulfate, phosphate, etc.), resulting in a negative ζ potential of about 30–50 mV in physiological buffer. Generally, despite their negative surface charge, these NPs are

immediately covered by plasma proteins when in contact with biological fluids, resulting in a significant reduction of their ζ potential to about 5–10 mV negative upon formation of the NP–corona complexes: thus, the colloidal stability of these complexes cannot be due to a pure electrostatic effect, but it is closely connected to the complex nature of the protein corona.⁴⁵ To inhibit opsonization, the surface of the NPs can be coated by suitable polymers such as polyethylene glycol (PEG) to reduce nonspecific binding and allow specific surface groups at the NP surface to bind specifically to receptors at cell surfaces.^{28,76–79}

3.7.2. Effects of Smoothness/Roughness. Surface effects can also be altered by nanoscale surface roughness (that is, local protrusions or depressions with radii smaller than that of the particle).^{23,80} Indeed, small-radius surface asperities dictate the strength of nanoparticle–cell interactions, likely as a result of differences in the composition of the corona shell on the surface of the NPs.²³ Simulations of NPs interacting with synthetic membranes suggest that nanoscale surface roughness greatly minimizes repulsive interactions (for example, electrostatic, hydrophilic), thereby promoting adhesion, which might translate into easier engulfment by cells.²³

3.7.3. Electron Transfer Capability. Electron transfer capability is mostly observed with TiO₂ and SiO₂ NPs, which are one of the most important categories of nanomaterials due to their wide use as electrochromic materials, catalysts, pigments, pharmaceuticals, food additives, sunscreens, and cosmetics.⁸¹ It is proposed that either electron confinement or the formation of electron–hole pairs at the surface of these NPs, could lead to severe damage of the structure of biomolecules and consequent generation of reactive oxygen species (ROS).^{82–86} For instance, cytotoxicity *in vitro* of TiO₂ NPs (mean diameter of 63 nm) to the human lung epithelial cell line A549 was probed.⁸⁷ DNA damage and oxidative lesions were determined using the Comet assay, and intracellular production of ROS was measured using the oxidation-sensitive fluoroprobe 2',7'-dichlorofluorescein diacetate (DCFH-DA). Results confirmed extensive DNA damage; however, little ROS was detected by DCFH-DA.⁸⁷ The toxic effect of TiO₂ NPs is size dependent, and by increasing their size from 63 to 200 nm, the absorption of proteins and Ca²⁺ ions (i.e., the presence of a divalent ion is found to be important for adsorption of proteins such as albumin and fibronectin)^{88–90} on the surface of TiO₂ NPs increased, leading to higher induced oxidative damage.^{91–95} Other reports indicate the production of ROS, glutathione depletion, and toxic oxidative stress caused by electron–hole pairs, photoactivity, and redox properties in semiconductor NPs, respectively.^{96,97} Therefore, when a protein is denatured on the surface of a NP, the exposure of new antigenic sites (cryptic epitopes) may initiate an immune response and can promote autoimmune disease.²³

The surface of TiO₂ NPs can be capped/coated by surfactants, polymers, complexing ligands, low-molecular-weight antioxidants, enzymatic scavengers, etc. to reduce the conformation changes in the protein upon adsorption.^{96,97}

3.7.4. Effects of Hydrophobicity/Hydrophilicity. A clear correlation between the affinities of biomolecules (e.g., proteins) for the surface of NPs and the extent of structural changes has been found.⁹⁸ Due to their high affinities for hydrophobic surfaces, adsorbed proteins can have a less native structure than when adsorbed on hydrophilic surfaces, leading to severe protein denaturation.⁹⁹ In addition, NP surfaces may take up proteins depending on their isoelectric points in a rather narrow pH range.¹⁰⁰ It has also been observed that an increase in

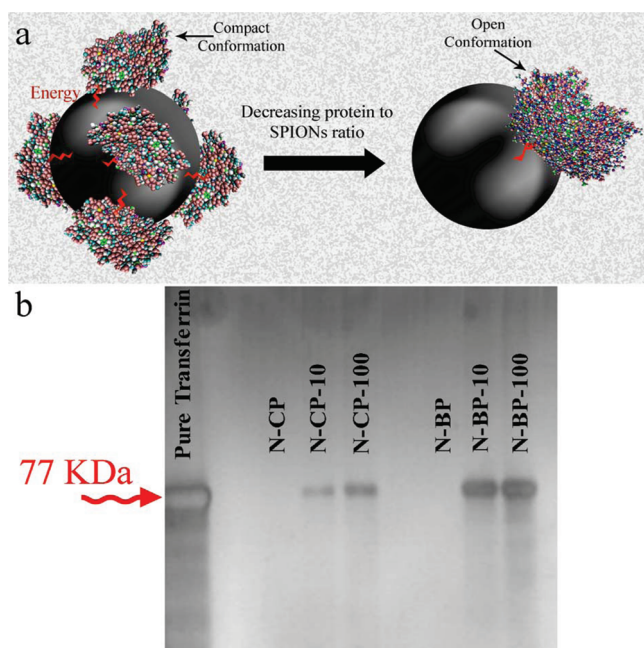


Figure 5. (a) Schematic representation of the effect of decreasing protein to SPION surface ratio on the conformation changes induced in human transferrin. (b) SDS–PAGE for human transferrin and remaining proteins on the surface of trapped bare and coated SPIONs (with various concentrations): N-CP (10–100), extract of the PVA-coated NPs from MACS after washing (PVA-coated NPs with a 10–100-fold increase in concentration (protein amount is constant); N-BP (10–100), extract of the bare NPs from MACS after washing (bare NPs with a 10–100-fold increase in concentration (protein amount is constant)). Reprinted with permission from ref 35. Copyright 2011 Royal Society of Chemistry.

electrostatic interaction is generally accompanied by a reduction of the modification of the native structure.¹⁰¹

According to literature reports, hydrophobic interactions tend to dominate the energy balance in most cases tested to date;^{12,24,102} however, the effect of electrostatic interactions cannot be ignored.¹⁰³ Cedervall et al. used ITC to show that the number of protein molecules bound (stoichiometry) increases with the particle hydrophobicity and that there was a clear difference in the protein affinities for polymeric particles of different hydrophobicities.¹²

3.7.5. Protein/NP Ratio. The concentration of NPs (i.e., protein/NP surface area ratio, r) also influences the binding properties (i.e., affinity). Lundqvist et al.²⁶ studied NP–protein complexes using several protein/NP ratios to optimize the characterization of the bio-nano interface; the results showed that the optimal protein solution to NP surface ratio for 50 and 100 nm polystyrene nanoparticles of various surface charges was at 2.8 mL/m². This is a necessary step for characterization using centrifugation to separate the NP–protein coronas from the unbound proteins, although the optimal ratio will depend on the nanoparticle density and the amount of proteins that bind to the nanoparticles.

Mahmoudi et al.⁵⁵ investigated the interaction of SPIONs with iron-saturated human transferrin using an optimized protein to NP surface ratio. To check the r effect, the concentration of SPIONs was increased 10- and 100-fold (decreasing r), leading to increased relaxation of the conformation of transferrin upon adsorption. The authors claimed that, by decreasing r , the number of proteins per NP is significantly decreased; therefore, more energy is transferred from the NPs to each protein molecule, resulting in a stronger

binding and more conformational changes of the proteins on the NPs (see Figure 5a). On the other hand, for the lower ratios, the stronger binding between protein and NPs does not allow the proteins to be released during the magnetic separation method (see Figure 2). To support this hypothesis, the authors used sodium dodecyl sulfate–polyacrylamide gel electrophoreses (SDS–PAGE) (Figure 5b). The results suggest that, by decreasing the r ratio, the protein amount on the surface of SPIONs (after separation of magnetic NPs with MACS) increased significantly, due to the enhancement of the binding energy between proteins and SPIONs. Interestingly, the SDS–PAGE bandwidths of the proteins were decreased for the poly(vinyl alcohol)-coated SPIONs in comparison with the bare ones. From the results, it was found that, besides the physicochemical properties of NPs, their concentration can have an important impact on the protein corona and the binding affinity and association/dissociation constants, although again the issue of how these effects hold up under competitive binding conditions remains to be addressed.³⁵ In addition, variation of the protein to NP surface ratio could change the composition of the corona. For instance, proteins such as HSA and fibrinogen may cover the surface of NPs for short periods of time, whereas lower abundance proteins with higher affinities and slower kinetics may ultimately displace them. On the contrary, by decreasing r , lower affinity binding proteins, such as albumin, may dominate the surface of NPs.^{12,23}

3.7.6. Effect of Functional Groups and Targeting Moieties. Ehrenberg and co-workers⁴⁵ used cultured endothelium cells as a model for vascular transport of polystyrene NPs with various functional groups (i.e., carboxyl, amidine, amine, lysine, cysteine, methyl, and PEG). According to the results (see Figure 6), the capacity of the various NP surfaces to adsorb proteins was indicative of their tendency to associate with cells. They concluded that NP–cell association was not reliant on the identity of the adsorbed proteins. Furthermore, quantification of the adsorbed proteins showed that high-binding NPs were maximally coated within seconds to minutes, indicating that proteins on the surface of NPs could mediate cell association over much longer time scales.

4. CONFORMATIONAL CHANGES OF PROTEINS UPON BINDING TO NPs

Lynch et al.¹⁰⁴ hypothesized that the function and fate of NPs in biological environments is related to the nature and composition of their surface protein corona; the protein-modified surface of NPs, with possible dysfunction of the bound proteins. Thus, the NP–protein complex interacts with the living system (e.g., cells, tissues, organs, etc.) rather than the bare NP surface, and this is a key phenomenon that scientists need to understand in order to develop smart nanomedicines and to ensure the safe implementation of nanotechnology. However, one of the significant challenges in this case is the determination of protein conformation changes after interaction with NPs and whether they are reversible or irreversible conformational changes. Since protein function is explicitly linked with protein conformation, understanding the type of conformational changes undergone by the proteins upon interaction with NPs is important, as the irreversible alteration of protein conformation is a recognized molecular mechanism of injury and can contribute to disease pathogenesis^{45,105–107} following protein dissociation from the surface of the NPs. The subsequent biological responses to the unfolded proteins are highly affected by their conformational changes. Therefore, a better understanding of the consequences

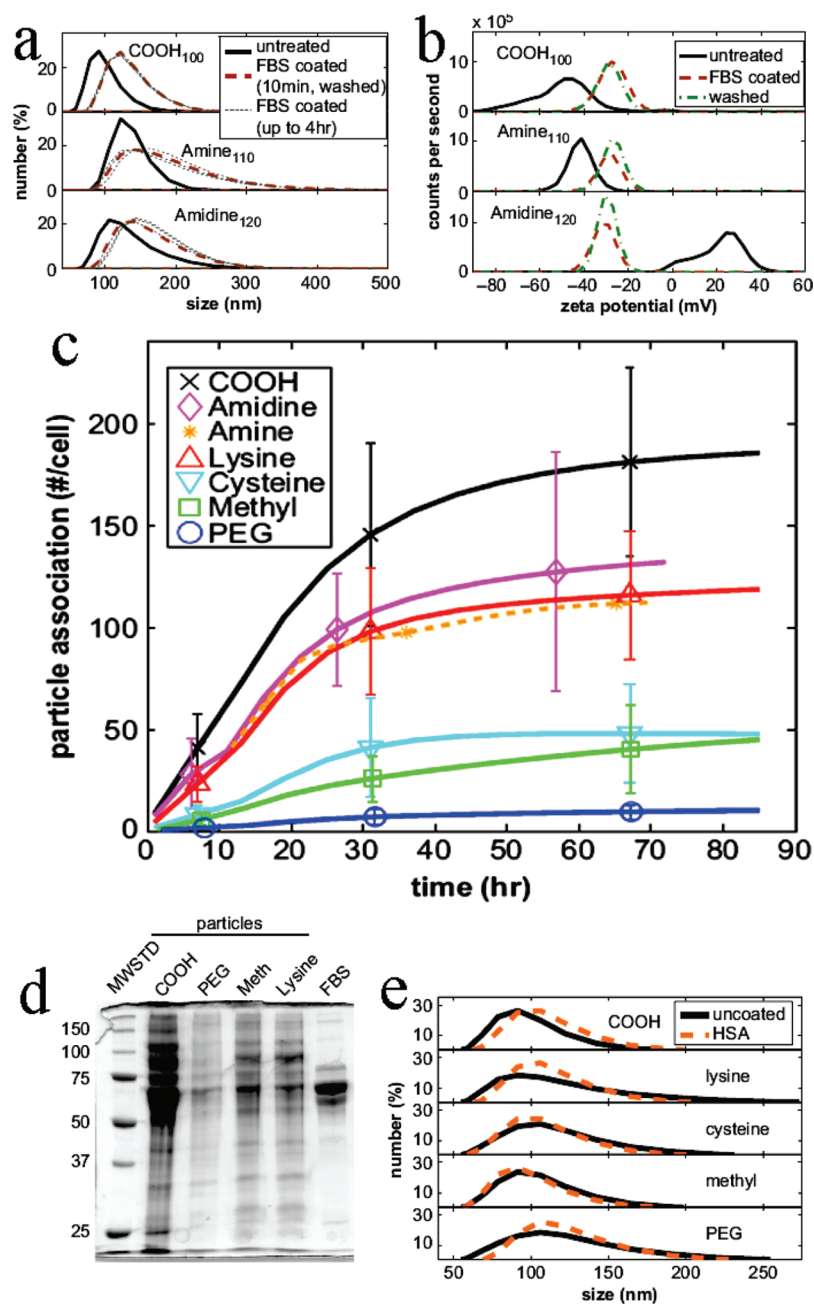


Figure 6. (a) Size enhancement (characterized by DLS; initial distributions are shown in solid black, the size after approximately 10 min in 25% fetal bovine serum (FBS) and washing is shown in dashed orange, and subsequent measurements after 2, 3, and 4 h are shown in dotted gray) and (b) shifts of the ζ potential (results shown in solid black initially, in dashed orange after 2 h in FBS, and in dashed-dotted green after a subsequent washing) due to the interaction of NPs with various surface functional groups with FBS proteins. (c) Association of NPs with various functional groups with cells over tens of hours. (d) Electrophoresis gel of the proteins from FBS adsorbed to the NP surface which demonstrates that particles with COOH functional groups adsorbed the most protein, PEG-coated NPs adsorbed the least protein, and methyl- and lysine-coated NPs adsorbed intermediate protein amounts. (e) Size measurements during HSA adsorption demonstrate an increase in size for all of the binding chemistries studied. Particle size distributions are initially shown in black and in dashed orange after adsorption of HSA. Reprinted with permission from ref 45. Copyright 2009 Elsevier.

of interaction with NPs on the protein conformation and activity is essential to develop functional as well as safe NPs.

4.1. Reversible Conformational Changes

The conformational changes of bovine serum albumin (BSA) in albumin–gold nanoparticle bioconjugates were investigated in detail by various spectroscopic techniques, including UV/vis absorption, fluorescence, circular dichroism, and Fourier transform

infrared spectroscopies.¹⁰⁸ The studies suggested that, upon physical adsorption to form BSA–gold bioconjugates, BSA underwent substantial conformational changes at both secondary and tertiary structure levels. BSA was found to adopt a more flexible conformational state on the boundary surface of gold nanoparticles. The conformational changes at pH 3.8, 7.0, and 9.0, at which different isomeric forms of albumin exist, were investigated to probe the pH effect on the conformation of BSA. The results showed that the pH of

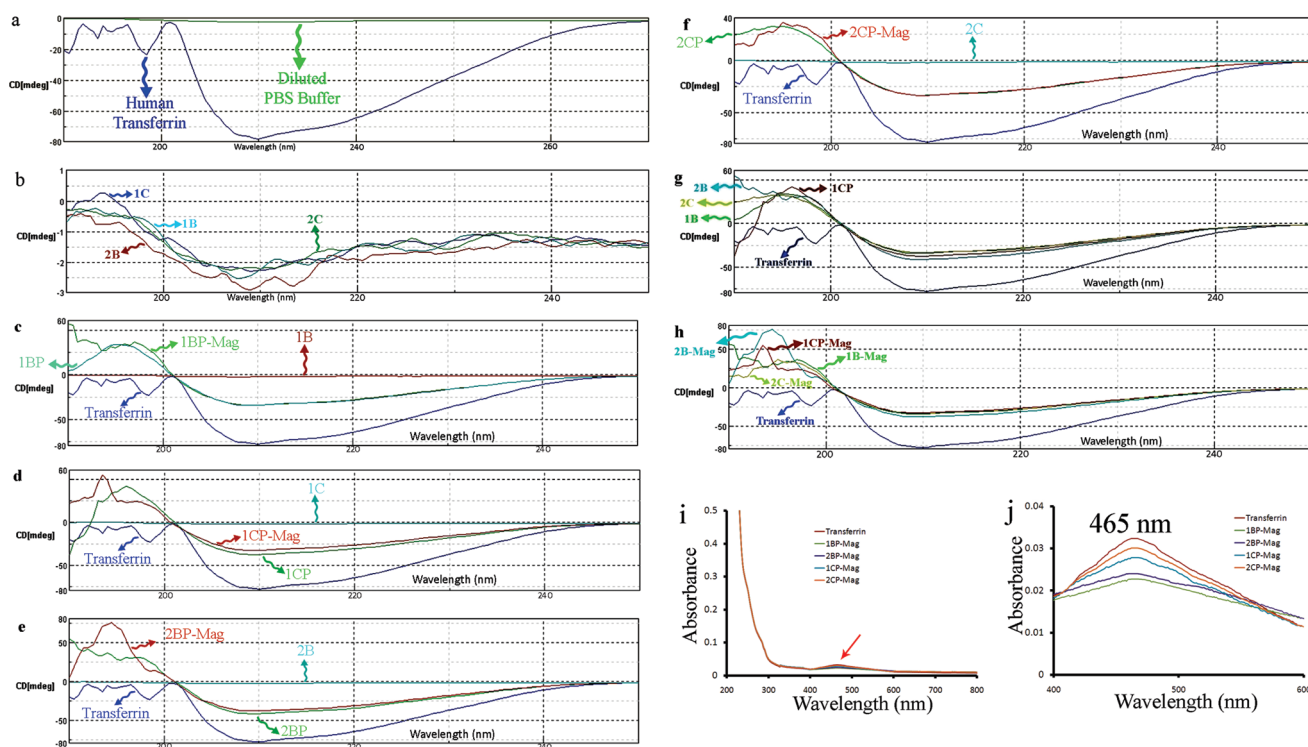


Figure 7. CD spectra of (a) pure human transferrin (iron-saturated) and buffer medium and (b) various magnetic NPs: pure human transferrin, SPIONs, suspension of transferrin and SPION NPs, and pure treated transferrin after MACS magnetic separation for the (c) 1B, (d) 1C, (e) 2B, and (f) 2C samples. Comparison of CD spectra of (g) suspensions containing transferrin and SPION NPs and (h) suspensions after MACS magnetic separation. UV/vis spectra (i) showing the absorbance changes associated with iron release for the SPION-treated transferrin due to its conformation changes and (j) showing the peaks of (i) in the 400–600 nm range. The numbers 1 and 2 are representative of smaller and larger NPs, respectively. Reprinted with permission from ref 35. Copyright 2011 Royal Society of Chemistry.

the medium greatly influenced the conformational changes, and fluorescence and circular dichroism studies further indicated that the changes were larger at higher pH. Dell'Orco et al.¹⁰⁹ developed a simple and effective dynamic model of the nanoparticle protein corona in a body fluid. The model predicts the time evolution and equilibrium composition of the corona on the basis of protein–surface affinities, stoichiometries, and association/dissociation rate constants. An application to the interaction of human serum albumin, high-density lipoprotein (HDL), and fibrinogen with 70 nm *N*-isopropylacrylamide/*N*-*tert*-butylacrylamide copolymer nanoparticles is presented.

$A\beta_{1-40}$ -coated 20 nm gold colloidal nanoparticles exhibit a reversible color change as the pH is externally altered between 4 and 10.¹¹⁰ This reversible process may contain important information on the initial reversible step reported for the fibrillogenesis of $A\beta_{1-40}$, which is a hallmark of Alzheimer's disease. The reversible color change was observed by microscopic investigations. AFM images on graphite surfaces revealed the morphology of $A\beta$ aggregates with gold colloids. Transmission electron microscopy (TEM) images clearly demonstrate the correspondence between the observed spectroscopic features and conformational changes of the protein, due to the presence of the gold colloid.

4.2. Irreversible Conformational Changes

The first study on conformational changes of a specific protein (i.e., human iron-saturated transferrin) due to interaction with SPIONs was reported by Mahmoudi et al.³⁵ Transferrin, with a molecular weight of 75000–80000 depending on the species, is a protein found in the blood of all vertebrate species.¹¹¹ Transferrin contains two iron-binding sites which appear to be equal and

independent in their iron-binding mode. As iron is bound to these sites, bicarbonate is bound to an anion-binding site in close proximity to each of the iron-binding sites, forming a red complex with an absorption at 465 nm.¹¹² Centrifugation has been used as the favored method to separate the NPs from the protein suspensions, which can affect the outcome by the duration of washing and the amount of solution volumes used in these steps.¹² However, the main problem of the centrifugation technique is the loss of the proteins which are adsorbed to the surface of NPs with weak binding.^{12,20} The distinguished feature of SPIONs is their superparamagnetic properties, which enable us to separate them without centrifugation, using external magnetic field gradients; hence, potentially more reliable results are obtained.³⁵

The various SPIONs (bare (with diameters of 5 and 8 nm) and PVA-coated (with diameters of 8 and 10 nm)) were incubated with pure human transferrin (iron-saturated).³⁵ The samples (see the descriptions in Table 1) were run on the MACS system (see Figure 2), and the various solutions were analyzed by circular dichroism (CD) to track the changes in protein conformation due to interaction with the magnetic NPs. The CD spectra of human transferrin confirm the existence of its closed compact conformation (Figure 7a). It is notable that the human serum transferrin is composed of two similar, but nonidentical, globular lobes, and each lobe (which bears an Fe(III)-binding site in a cleft between its domains)^{113,114} is divided into two domains consisting of β -sheets overlaid with α -helices.^{115–117} By releasing the iron from the transferrin structure (apotransferrin), the compact conformation is relaxed; more specifically, the two

Table 1. Description of Sample Abbreviations^a

sample	description
B	bare NPs
C	PVA-coated NPs
BP	protein interacted with bare NPs
CP	protein interacted with PVA-coated NPs
BP-Mag	extract of the interacted proteins with bare NPs using MACS
CP-Mag	extract of the interacted proteins with PVA-coated NPs using MACS
BP-KCl	washing of the trapped bare NPs in MACS with 1 M KCl solution
CP-KCl	washing of the trapped PVA-coated NPs in MACS with 1 M KCl solution
N-BP	extract of the bare NPs from MACS after washing
N-CP	extract of the PVA-coated NPs from MACS after washing
BP-10	using bare NPs with 10-fold increased concentration (protein amount is constant)
CP-10	using PVA-coated NPs with 10-fold increased concentration (protein amount is constant)
BP-100	using bare NPs with 100-fold increased concentration (protein amount is constant)
CP-100	using PVA-coated NPs with 100-fold increased concentration (protein amount is constant)

^a Reprinted with permission from ref 35. Copyright 2011 Royal Society of Chemistry.

domains of each lobe achieve an open jaw conformation.¹¹⁸ CD spectra of the diluted phosphate-buffered saline (PBS) and all SPIONs (Figure 7b) show curves near the zero baseline, thus confirming their negligible effect on the CD spectra. According to the CD spectra (Figure 7c–h), by introducing SPIONs to a transferrin solution, the conformation of the iron-saturated protein is changed. The significant decline in peak intensity at a wavelength of around 210 nm for the NP-bound proteins confirms the opening of the compact transferrin conformation. After removal of the magnetic NPs using the MACS system, the conformation of pure treated proteins is not recovered, showing the irreversible changes in transferrin conformation after interaction with the SPIONs (Figure 7h). The UV/vis spectra of the pure transferrin and SPION-treated transferrin after removal of SPIONs are illustrated in Figure 7i,j. The characteristic peak at a wavelength of 465 nm is due to the iron-bearing lobes of iron-saturated transferrin. Therefore, the release of iron from the two tyrosine ligands causes a decline of the peak.^{119,120} According to the CD curves, the exposure of iron-saturated human transferrin to SPIONs results in the release of iron, and more specifically, it changes the compact conformation of transferrin to the open conformation of the iron-free lobe. Furthermore, the decline of the characteristic peak of the transferrin (at 465 nm) is dependent on the size and surface properties of the SPIONs. For instance, the most significant protein conformational changes are obtained upon interaction with the bare NPs (i.e., Figure 7j). The PVA-coated NPs cause less conformation change in transferrin, probably due to their lower surface energy in comparison to the bare magnetic NPs; the same effect of the size of the SPIONs are detected in coated NPs. According to the results, the authors confirmed that the exposure of iron-saturated human transferrin to the SPIONs results in the release of iron, which caused irreversible changes to the main function of this protein, i.e., the transport of iron among cells.³⁵ Furthermore, transferrin changes from a compact to an open conformation. After removal of the magnetic NPs, the original protein conformation is not recovered, indicating irreversible changes in the transferrin conformation after interaction with the SPIONs.

5. ANALYTICAL METHODS FOR CORONA EVALUATION

Upon contact with biological fluids (serum, plasma, lung lining fluids, etc.), NPs interact strongly with proteins and other

biomolecules, which dramatically change their surface properties. Thus, the NP's surface acquires a new biological identity which most likely will influence its stability and interaction with living matter affecting the nanoparticle biodistribution in *in vivo* experiments. For example, the adsorption of opsonins, such as immunoglobulins, complement proteins, fibrinogen, etc., can enhance the phagocytosis with immediate removal of the particles from the bloodstream, while the adsorption of proteins, such as serum albumin and apolipoproteins, and other protein carriers of the bloodstream, can elongate NP circulation. Moreover, protein adsorption onto curved NP surfaces may induce conformational changes of the protein native structure with possible exposure of novel epitopes which may transmit biological signals.¹² The resulting perturbed signaling transduction in cells may have adverse effects on cellular function and cause toxicity *in vitro* and *in vivo*. Therefore, it is essential to apply and develop analytical methods with new protocols to investigate NP–protein interactions in order to understand the mechanistic basis for the possible biological activity of these complexes and to achieve a safety assessment of the nanomaterials used for biological applications. Li et al.¹²¹ summarized recent progress in the development of analytical strategies to investigate NP–protein interactions.

When nanomaterials are meant for biological applications, it is necessary to investigate their physicochemical properties in the biological milieu. As explained earlier, many studies have been performed to shed light on the protein–NP association/dissociation processes in serum, plasma, etc. The determination of binding rates, affinities, and stoichiometries of protein association with, and dissociation from, nanoparticles in biological fluids is particularly complex since more than 3700 proteins in different concentrations coexist and compete for binding to the NP's surface. Recently, both gold NPs and quantum nanodots have been shown to give unique optical profiles with a shift of the typical surface plasmon resonance (SPR) peak in protein solutions. This shift has been related to the modification of the surface environment upon protein adsorption. Similarly, the increase of the NP hydrodynamic diameter measured by photon correlation spectroscopy (PCS) also provides evidence of protein adsorption.^{122,123}

One strategy commonly used to prevent unwanted protein adsorption is to coat the NP's surface with long polymer chains such as PEG.¹²⁴ Similarly, other surface-immobilized biomolecules,

such as proteins, polysaccharides, and lipids, may be used to reduce nonspecific protein adsorption and therefore unwanted biorecognition of nanosystems.

5.1. Spectroscopy Methods

5.1.1. UV/Vis. Protein binding to NPs induces changes in the absorption spectra of the NP or proteins, and these changes can be used to evaluate the binding.^{69,108,125–136} The shift and broadening of the absorption spectra of the NP–protein complex depend on the NP size and aggregation state and the local dielectric environments.^{127,130} For example, it was shown that the red shift and the widening of the peak in the absorption spectra of azurin (Az)–gold NP solutions depend on the Az concentration. UV/vis spectroscopy can thus be used to analyze NP–protein binding, although quantitative and conclusive results are difficult to achieve. In fact, protein–nanoparticle complexes are characterized by a different size distribution compared to the bare nanoparticles, with possible formation of NP–dimer and NP–trimer conjugates, which will give a different scattering contribution to the overall absorption spectra. Compared with other methods, UV/vis is faster, more flexible, and less complicated, but it is not conclusive and needs to be performed in association with other complementary spectroscopic and structural investigations.

5.1.2. Fluorescence. Labeling proteins with fluorescent probes allows the use of fluorescence spectroscopy to study their structural and dynamic properties. The fluorescent labeling has to be well designed to avoid introducing major conformational changes to the native structure of the protein. Moreover, we can also argue that the addition of a dye can affect the interaction of the protein with the NP, if the dye has higher affinity for the NP surface than the protein's functional groups. Fluorescence spectroscopy is sensitive to protein dynamics because the excited fluorescent state persists for nanoseconds, which is the time scale of many important biological processes, such as the rotational motion of protein side chains, molecular binding, and conformational changes.^{66,108,130,137–148} When NPs are intrinsically luminescent or labeled with fluorescence probes,¹⁴⁷ fluorescence emission can also be detected from the NPs. NP–protein binding can be monitored by steady-state or time-resolved fluorescence spectroscopy,^{108,130,138,141–146,148} fluorescence resonance energy transfer (FRET),^{66,149,150} or stepwise single-molecule photobleaching.¹⁵¹ Intrinsic protein fluorescence from Trp groups can also be used to monitor changes in the protein microenvironment upon binding to NPs.

Recently, fluorescence correlation spectroscopy (FCS) has been used to study the interaction between proteins and NPs in a physiological buffer. FCS measures the intensity of fluorescently labeled particles in a very small confocal volume. When a labeled NP passes into or out of that volume, a change in the measured fluorescence is observed, and therefore, the time taken for the particle to traverse the volume can be measured, assuming Stokes–Einstein diffusion structural information regarding the object can be extracted.

Rocker et al.¹⁰⁷ have elegantly analyzed the adsorption of human serum albumin onto small (10–20 nm) polymer-coated FePt and CdSe/ZnS NPs using FCS, showing the formation of a protein corona monolayer with a thickness of 3.3 nm. They have also performed a time-resolved fluorescence quenching study, showing that the proteins bind to the negatively charged NPs with micromolar affinity and reside on the particle for ~100 s. Jiang et al. have quantitatively analyzed the adsorption of human

transferrin onto small polymer-coated FePt NPs also using FCS.¹⁵² Here, transferrin was shown to bind to the negatively charged NPs with an affinity of approximately 26 mM in a cooperative fashion and to form a monolayer with a thickness of 7 nm. Thus, it appears clear that FCS has potential to be used in the future to obtain quantitative data on the dynamics of the protein corona in a biological environment, which would be useful for a multitude of protein (nano)science applications. This, surely, implies further development of the methodology and the design of experiments with both nanoparticle and protein fluorescent labels so that cross-correlation fluorescence spectroscopy could help to shed light on the dynamics of association/dissociation to and from NP surfaces.

5.1.3. Fourier Transform Infrared and Raman Spectroscopy. Vibrational spectroscopies, Raman and Fourier transform infrared (FTIR), can be useful methods to get information about the surface properties of NP–protein complexes and to detect protein binding onto the NP surface. Although both techniques investigate vibration modes, they give complementary information. In fact, they have different selection rules and specific advantages and disadvantages for biological applications. Generally, the usual experimental problem associated with vibrational spectroscopy of a protein is spectral crowding. However, resonance Raman or isotope editing, among other approaches, yields unambiguous structure-specific assignments.¹⁵³ There are two main advantages of Raman over FTIR for studying NP–protein interactions: its ability to measure the protein–NP complexes in aqueous solution and the greater spectral simplicity in Raman spectra than IR spectra because the localized vibrations of double or triple bonds or electron-rich groups generally produce more intense Raman bands than the vibrations of a single bond or electron-poor groups.¹⁵⁴ FTIR has been used to monitor the structure of NP-bound proteins,^{66,129,155–157} and the protein secondary structures are estimated on the basis of the absorption of amide bonds. Among the amide I, II, and III bands, the amide I vibrational band (1700–1600 cm⁻¹) is the most sensitive and is frequently used to determine protein conformation. Raman spectra of proteins consist of bands associated with the peptide main chain, aromatic side chains, or sulfur-containing side chains.^{154,158} For example, the interaction between human hemoglobin (Hb) and bare CdS quantum dots (QDs) has been investigated.¹⁵⁸ The spin state of the heme iron of Hb does not change by binding to the surface of the CdS QDs, but the binding induces an orientation change of heme vinyl groups from in-plane or close to in-plane to out-of-plane.¹⁵⁸ Not only are these spectroscopic methods used to detect conformational changes, they also confirm the protein attachment onto NPs through the appearance of additional characteristic bands.

5.1.4. Circular Dichroism. Different protein secondary structures (α -helix, β -sheet, etc.) have their own characteristic CD spectra in the UV region. This method has been widely used for monitoring conformational changes induced by protein–NP interactions.^{66,69,86,125,129,131,138,140,143,146,159–163} NPs are not usually chiral in nature and thus do not affect the protein CD spectra, although, if their size is large, they can give a scattering contribution which can affect the CD signal. The approximate fraction of a specific secondary structure present in the protein can thus be determined by analyzing its far-UV CD spectrum as a sum of fractional multiples of reference spectra typical of the secondary structural type. Like all spectroscopic techniques, the

CD signal reflects an average of the entire molecular population. Thus, while CD can determine if a protein contains about 50% α -helix, it cannot determine which specific residues are involved in the α -helical portion. The CD spectrum of a protein in the “near-UV” spectral region (250–350 nm) can be sensitive to certain aspects of tertiary structure. At these wavelengths the active chromophores are the aromatic amino acids and disulfide bonds, whose CD signals are sensitive to the overall tertiary structure of the protein. In particular, signals in the 250–270 nm region are attributable to phenylalanine residues, in the 270–290 nm region to tyrosine, and in the 280–300 nm region to tryptophan. Disulfide bonds give rise to broad weak signals throughout the near-UV spectrum. The near-UV CD spectrum can be sensitive to small changes in tertiary structure due to protein–protein interactions and/or changes in solvent conditions. Although CD cannot be applied on complex protein mixtures, it can provide useful information on protein structure changes resulting from adsorption to a NP surface.

5.1.5. Nuclear Magnetic Resonance. Hellstrand et al.¹⁶⁴ showed, using size-exclusion chromatography and nuclear magnetic resonance (NMR), that copolymer NPs bind cholesterol, triglycerides, phospholipids and lipoproteins from human plasma and that the binding reaches saturation. The lipid and protein binding patterns correspond closely to the composition of HDL. By using fractionated lipoprotein complexes, they also showed that HDL binds to copolymer NPs with much higher specificity than other lipoprotein complexes (LDL, VLDL). Apolipoproteins have been identified as strong binders to many other NPs, suggesting that lipid and lipoprotein binding is a general feature of NPs under physiological conditions, possibly as a result of the similar size range and curvatures of NPs compared to the naturally occurring lipoprotein complexes which have sizes in the range of 8–100 nm.¹⁶⁴

Stayton et al.¹⁶⁵ have utilized solid-state NMR to provide *in situ* secondary-structure determination of statherin peptides on biologically relevant hydroxyapatite (HAP) surfaces. In addition to enabling a direct structural study, molecular dynamics studies have provided considerable molecular insight into the protein-binding footprint on hydroxyapatite. This also led to the design of biomimetic fusion peptides that utilize nature’s crystal-recognition mechanism to display accessible and dynamic bioactive sequences from the HAP surface.

5.2. Other Methods

5.2.1. Dynamic Light Scattering. In dynamic light scattering (DLS) experiments, the normalized time autocorrelation function $g_2(q, t)$ of the scattered intensity is measured according to

$$g_2(q, t) = \frac{\langle I^*(q, 0) I(q, t) \rangle}{\langle I(q, 0)^2 \rangle} \quad (1)$$

For ergodic systems, this function can be expressed in terms of the field autocorrelation function $g_1(q, t)$ through the Siegert relation

$$g_2(q, t) = A[1 + \beta^2 g_1(q, t)^2] \quad (2)$$

where A is the baseline and β^2 is the coherence factor, which is dependent on the scattering geometry and details of the detection system. When the spectral profile of the scattered light can be described by a multi-Lorentzian curve, then $g_1(q, t)$ can be

written as the Laplace transform of the spectrum of relaxation times:

$$g_1(q, t) = \int_0^\infty w(\tau) e^{-t/\tau} d\tau \quad (3)$$

where τ is the relaxation time characteristic of the system and $w(\tau)$ is its weight factor in the relaxation time distribution. To obtain a distribution, $w(\tau)$, of decay rates, a constrained regularization method, CONTIN, developed by Provencher²⁷ is used to invert the experimental data. If the motion of a nanoparticle is diffusive, it is possible to calculate the translational diffusion coefficient, D_c , from the relaxation time. It is commonly agreed that D_c provides access to the hydrodynamic size, d_H , through the Stokes–Einstein relationship $D_c = K_B T / 6\pi\eta_s d_H$, for spherical NPs, with η_s being the solvent viscosity and K_B the Boltzmann constant.

Thus, DLS experiments give access to the particle hydrodynamic size distribution through an inverse Laplace transform of the autocorrelation intensity function.

When proteins bind to the NP surface, the size of the NP increases, changing its Brownian motion, which can be detected by DLS. DLS has also been used to monitor the binding ratio of protein–NP complexes, since the increase in the hydrodynamic size stops when the binding is saturated.^{66,127,134,166–169} Nonetheless, scattering data are dominated by the contributions from larger objects since the intensity increases as R_H^6 , so for polydisperse systems, the particle size distribution is shifted towards larger size and the amplitudes of the populations are not reliable. The hydrodynamic diameters from DLS represent the sizes of the objects moving in the solution and include the hydration and counterion shells and are generally larger than the sizes obtained by microscopy.¹⁶⁸ Some of the newer instruments released into the market are designed to be used also by a nontrained user, allowing easy access to the machine. DLS measurement requires very clean samples (dust contamination can significantly alter the results), dilute samples, and a monodisperse population. In summary, DLS represents a fast, cheap, and somewhat reliable method to measure the size distribution of NP–protein complexes in physiological buffers and to detect possible aggregation issues.

Sometimes, NP dispersion in a biological environment results in some aggregation or a shift in the particle size distribution. Such unexpected aggregation can have a significant effect on the available nanoparticle dose and on interpretation of any results obtained thereafter in terms of NP interactions with living systems. Unlike classical light-scattering techniques, the nanoparticle tracking and analysis (NanoSight NTA) technique allows nanoparticles to be sized in suspension on a particle-by-particle basis, allowing higher resolution and therefore better understanding of aggregation than ensemble methods (such as DLS). Montes-Burgos et al. showed how the NTA technique can be extended to multiparameter analysis, allowing for characterization of the particle size and light scattering intensity on an individual particle basis, including in the presence of plasma.¹⁷² This multiparameter measurement capability allows subpopulations of nanoparticles with varying characteristics to be resolved in a complex mixture. Changes in one or more of such properties can be followed both in real time and *in situ*.

5.2.2. Isothermal Titration Calorimetry. Isothermal titration calorimetry (ITC) can be used to directly measure the binding affinity constant, enthalpy changes, and binding stoichiometry between NPs and proteins in solution.^{25,44,66,170,171} On

the basis of the measurement of small changes of temperature, Gibbs energy and entropy changes can be easily calculated. To quantify protein binding as a function of the NP characteristics, typically a protein is titrated into the NP solution and the heat response is recorded. The heat changes are then fitted to the isothermal function, and thermodynamic parameters are obtained. In a study of QD–HSA interaction, the thermodynamic parameters of the system were calculated at different temperatures. Results indicated that electrostatic interactions played a major role in the binding reaction because negative enthalpy and positive entropy values were obtained.⁶⁶

Cedervall et al.¹² showed that ITC is suitable for studying the affinity and stoichiometry of protein binding to NPs. Lindman et al.,²⁵ further showed that ITC is a straightforward method for measuring protein adsorption to nanoparticles in a quantitative manner. In particular it can be used to derive specific effects driving adsorption and give accurate degrees of adsorption and provide good complement to more qualitative or structural methods.

5.2.3. ζ Potential. Many nanoparticles in solution bear an electrostatic charge on their surface that hampers the inter-particle interaction/aggregation by electrostatic repulsion. However, ions and ionic surfactants in the solution can adsorb onto the NP surface, modifying the overall surface charge and forming an electrical double layer around each particle. This consists of an inner layer, called the Stern layer, more strongly bound to the surface and an outer diffuse layer less firmly bound to the NP surface. Within the diffuse layer, there is a boundary, the slipping plane, inside which the ions and particles form a stable entity (and travel together under an electrical field), and the ζ potential measures the electric potential at this slipping plane. Generally, NPs characterized by a large ζ potential repel each other and do not flocculate, thereby forming a stable dispersion. Thus, the ζ potential gives information on the surface charge of the NPs and can be used to detect protein binding to the NP surface as this will change the overall surface charge. For example, the interaction of negatively charged BSA and positively charged lysozyme with a range of metal oxide particles (such as alumina, silica, titania, or zirconia) was studied by ζ potential measurements.³⁶ The adsorbed proteins changed the ζ potentials and the isoelectric points of the oxide particles.³⁶

Lundqvist et al.²⁶ studied the protein corona formed from human plasma for a range of NPs that differ in surface properties and size. Six different polystyrene NPs were studied: three different surface chemistries (plain polystyrene, carboxyl-modified polystyrene, and amine-modified polystyrene) and two sizes of each (50 and 100 nm), enabling the authors to perform systematic studies of the effects of the surface properties and size on the detailed protein coronas. They concluded that both the size and surface properties play a very significant role in determining the coronas on the different NPs of identical underlying material composition.

5.2.4. Differential Centrifugal Sedimentation. Walczyk et al.⁴⁸ have studied the structure and stability of protein–NP complexes in human plasma and those washed free of excess plasma (leaving the so-called hard corona complexes) to understand the strength of binding of the corona and thus its impact on the interaction of NPs with living matter. Using a method called differential centrifugal sedimentation (DCS), they determined that the protein corona is about 10 nm thick for some nanomaterials (e.g., polystyrene and silica), and once the corona has

formed and equilibrated, this thickness does not change with time. DCS is probably one of the few techniques that allows measurement of the size distribution of NP–protein complexes in a semiquantitative way in the presence of the complex protein mixture, i.e. *in situ*. Particles differing in size by less than 5% can be resolved as single peaks, allowing distinction between protein–NP monomers, dimers, and trimers which would not be discriminated with DLS. Moreover, the possibility to measure NP–protein complexes in the biological fluid enables comparison of their size distribution to that of complexes free of excess plasma to understand if they are representative of what occurs in the biological milieu.

5.3. X-ray Crystallography

X-ray crystallography is now used routinely to determine how a drug interacts with its protein target and what changes in the drug structure might improve this.^{173,174}

In a recent study,¹⁷⁴ diastase enzyme was immobilized on nickel-impregnated silica paramagnetic NPs and characterized using Fourier transform infrared spectroscopy and X-ray crystallography. Analysis of the nature of enzyme binding with these NPs under different physiological conditions revealed that the binding pattern and activity profile varied with the pH of the reaction mixture. The immobilized enzyme was further characterized for its biocatalytic activity. Paramagnetic nanoparticle-immobilized enzyme showed a higher affinity for the substrate than the free enzyme.

5.4. Chromatography

Size Exclusion Chromatography (SEC), also known as gel filtration chromatography, is an old and versatile technique routinely used in chemical and biological laboratories to separate chemical compounds, polymers, or biological polymers, such as proteins, polysaccharides, and nucleic acids, on the basis of their size. There are several stationary phases (e.g., dextran, agarose, and polyacrylamide) that allow separation of biomolecules in different size ranges.^{24,69,137,140} Besides separating bound proteins, SEC is also able to detect the preferential binding and exchange rate during NP–protein interactions. Such properties can be analyzed on the basis of the elution profile of proteins.¹² Each protein is eluted with a characteristic volume depending on its molecular weight. In the presence of NPs, the elution volume of proteins is smaller following interaction between the protein and the NP, as the NPs elute in the void volume, being too large to enter the pores of the separation phase. This approach is particularly useful when the NPs have an electrostatic interaction with the stationary phase.

In reversed-phase chromatography (RPC) and ion exchange chromatography (IEC) biomolecules, mainly proteins and peptides, are separated on the basis of different retention times resulting from their hydrophobicity (RPC) and their charge (IEC).^{125,166} RPC requires a polar stationary phase on which a nonpolar domain adsorbs, and proteins are progressively eluted by injecting a linear gradient of polar mobile phase. IEC separation is based on Coulombic attraction between the biomolecule and the stationary phase, and the bound substances are progressively eluted by applying a buffer gradient with high ionic strength. On the basis of the charge of the matrix IEC, positively or negatively charged molecules are retained and subsequently eluted by applying a linear gradient of high salt concentration. As the protein charge status depends on the pH of the solution (molecules have a positive charge below their isoelectric point and a negative charge above it), the pH of the mobile phase has to

be carefully monitored. Although this technique has been largely used for protein purification from a complex mixture, it is now routinely coupled with mass spectrometry. By adjusting the pH or ionic concentration of the mobile phase, various protein molecules and NP–protein complexes can be separated. IEC includes cation exchange chromatography and anion exchange chromatography: the former retains cations (positively charged proteins or NP–protein complexes) using a column of negatively charged beads; the latter retains anions using positively charged beads. For example, IEC was used to separate gold NPs (Au NPs) with various peptide cappings.¹⁷⁵

5.4.1. Electrophoresis. Electrophoresis is the most widely used method for the separation and analysis of complex protein mixtures, where charged molecules dispersed in a fluid migrate under an electric field. Capillary electrophoresis (CE) and gel electrophoreses (one-dimensional gel electrophoresis (1-DE) and two-dimensional gel electrophoresis (2-DE)) are commonly used for analyzing NP–protein complexes.

5.4.1.1. Capillary Electrophoresis. CE separates proteins on the basis of their charge and frictional forces.^{176,177} Separation by CE can be detected using UV or fluorescence detection. CE was used to study the adsorption of the major plasma protein albumin onto poly(methoxypolyethylene glycol cyanoacrylate-co-hexadecyl cyanoacrylate) (PEG-PHDCA) NPs. CE allowed the direct quantification of adsorbed proteins without the requirement for a desorption procedure.¹⁷⁷ However, one drawback of CE is that proteins are easily adsorbed onto the inner surface of the capillary, and as such the detection sensitivity is not high.

5.4.1.2. One-Dimensional Gel Electrophoresis. SDS–PAGE is probably the most common technique in several laboratories, where protein mixtures are separated by molecular weight under an electric field.^{24,26,141,157,178–181} The proteins migrate through a vertical gel of acrylamide cross-linked with bisacrylamide and are separated according to their size due to their different electrophoretic mobilities. The proteins must be denatured and negatively charged, which can be achieved simply by boiling them with a reducing agent (dithiothreitol (DTT) or β -mercaptoethanol) and an anionic detergent (SDS). While the reducing agent will only reduce the disulfide bonds within cystine residues, SDS denatures the proteins by binding to the amino acids, causing electrostatic repulsion and thus protein unfolding. The same recipe has been successfully applied to denature and detach proteins adsorbed onto NP surfaces. The negative charge of the proteins given by SDS causes protein repulsion and thus detachment from the NP surface. The proteins resolved in the gel can be stained with one of several available stains (Coomassie brilliant blue, silver nitrate staining, deep purple, etc.), and densitometry analysis is routinely used to quantify protein abundance.²² SDS–PAGE is an extremely quick, cheap, and reliable technique that allows up to 14 protein coronas from different samples to be resolved simultaneously within the same gel. Although it has several advantages, it suffers from poor protein separation if the protein complex is too rich, resulting in comigration in the same gel bands of several proteins.

5.4.1.3. Two-Dimensional Gel Electrophoresis. 2-DE is a powerful and common technique for large-scale studies in proteomics where more than 5000 proteins can be separated within the same gel.^{51,176,177,182,183} The proteins are separated in two steps or dimensions. In the first dimension the proteins are separated according to their charge by isoelectric focusing (IEF) and in the second dimension are further separated according to their size (molecular weight) by SDS–PAGE.

After the proteins are separated, a staining method must be used so that the protein spots can be visualized in the gel and converted into a digital image. An ideal staining method should be sensitive enough to detect low-abundance proteins in the sample and also have a linear dynamic range throughout all the spots of different intensity in the gel. Such a linear dynamic range ensures that the spot intensity is linearly correlated with the protein abundance. Additionally, if the staining is compatible with protein identification, the spot of interest can be excised directly from the gel and analyzed to obtain the identities of the protein spots of interest.

While Coomassie blue staining suffers from low sensitivity,¹⁸⁴ ammoniac silver staining and several of the fluorescent approaches ensure high sensitivity, detecting less than 1 ng of proteins, and also have a linear dynamic range of intensity of 4 orders of magnitude,^{185,186} ensuring high quality and reliable results. Another attractive approach is difference in gel electrophoresis (DIGE), which uses cyanine fluorophore dyes (CyDyes) that covalently bind proteins in a complex mixture prior to IEF and 2-D PAGE. There are now three dyes available with the same mass and charge but differing in their emission and excitation spectra. They are also extremely bright so that only 3–5% of the protein needs to be labeled. A typical DIGE experiment requires the labeling of each individual sample with one of the three CyDyes, and then three samples are pooled and run on a 2-D gel. After the protein migration is performed, the gel is scanned using a fluorescent scanner, obtaining three different images from the same gel using the emission and excitation settings for each of the three CyDyes.¹⁸⁷ This approach is particularly attractive because if two sample conditions are run in the same gel, it is possible to identify spot changes, thereby reducing any error that is caused by running samples in different gels. After image capture, the gel images have to be imported into an image analysis software which quantifies the spot intensity and compares spot abundances from different gels, and the matching of the same spots across the gels, which can be quite challenging. Gel spots that are significantly different between gels can be analyzed afterward by mass spectrometry to obtain the protein identity.

Because it is unlikely that two molecules are similar in two distinct properties, molecules are more effectively separated in 2-DE than in 1-DE. Plasma and serum proteins bound to poly(D, L-lactic acid) (PLA) NPs were analyzed by 2-D PAGE.⁵¹ Protein bands on a scanned image of 1-DE gel or protein spots on a scanned image of 2-DE gel could be determined to quantify individual proteins. Because of more effective separation, 2-DE is more suitable for quantitative analysis.

Gessner et al.¹⁸⁸ investigated changes in the plasma protein adsorption patterns resulting from surface hydrophobicity variation. Latex particles with decreasing surface hydrophobicity were synthesized as model colloidal carriers. Physicochemical characterization was performed, and considerable differences in the protein adsorption patterns on the particles were detected using 2-D PAGE.¹⁸⁸

Although the 2-D gel technique provides reproducible protein migration in a gel and protein identities can be obtained relatively quickly, obtaining high gel quality can be quite time-consuming, has several technical difficulties, and requires specific equipment especially if using fluorescent staining approaches, and the image analysis to obtain spot changes within gels is quite expensive. Spot matching is also a difficult and time-consuming job and is prone to human error.

5.4.2. Mass Spectrometry. While in the past mass spectrometry (MS) has been predominantly used for chemical analysis,

Table 2. List of the Principal Analytical Methods To Study Protein–NP Interactions and Their Advantages and Disadvantages

analytical method	advantages	disadvantages	refs
UV/vis	cheap, fast, flexible, and simple; little sample preparation	nature of the solvent, pH of the solution, temperature, high electrolyte concentrations, and presence of interfering substances can influence the absorption spectrum; experimental variations such as the slit width (effective bandwidth) of the spectrophotometer will also alter the spectrum; to apply UV/vis spectroscopy to analysis, these variables must be controlled or accounted for to identify the substances present unstable	69, 128, 136, 194
fluorescence spectroscopy	sensitive		108
FTIR	quite cheap, versatile, easy to identify functional groups; sensitive to protein conformation; not constrained by substrate size or material	sample characterization is not possible in complex media; cannot get fine structural detail; time-consuming sample preparation; sample preparation destroys the sample	65
Raman spectroscopy	can be used with solids and liquids; no sample preparation needed; no interference from water; nondestructive; highly specific—like a chemical fingerprint of a material; Raman spectra are acquired quickly (within seconds); samples can be analyzed through glass or a polymer packaging; laser light and Raman scattered light can be transmitted by optical fibers over long distances for remote analysis; Raman spectra can be collected from a very small volume (<1 μm in diameter); inorganic materials are normally easily analyzed by Raman compared to infrared spectroscopy	cannot be used for metals or alloys; Raman effect is very weak; detection needs a sensitive and highly optimized instrumentation; fluorescence of impurities or of the sample itself can hide the Raman spectrum; sample heating through the intense laser radiation can destroy the sample or cover the Raman spectrum	154, 195
mass spectrometry	high-resolution method for characterization of NP-bound proteins; unique technique to obtain protein identities	expensive; requires dedicated facility and trained user	196
NMR spectroscopy	can detect very fine structural components; works for organic and inorganic materials; qualitative and quantitative, versatile; it can be applied to a wide variety of samples for direct structural study and molecular dynamics studies, both in solution and in the solid state	expensive, time-consuming; spectra take a long time to interpret	
DLS	nonperturbative, fast, and accurate, giving a measure of the vesicle hydrodynamic diameter as this dimension changes in solution	hydrodynamic diameters are influenced by the formation of hydration shells, the shape of the particles, and counterion binding; requires a monodisperse population	69
CD	monitoring conformational changes induced by protein–NP interaction	inherent inconsistency problems in absolute secondary structure determination; CD signal reflects an average of the entire molecular population; CD measurements cannot provide information regarding local structural alterations at the level of individual amino acids requires relatively high concentrations of samples	25, 44
ITC	can directly and quantitatively measure the binding affinity constant, enthalpy changes, and binding stoichiometry between NP and proteins in solution; no labeling or immobilization is required; not limited by the ligand or protein size; relatively artifact-free and not affected by the optical properties of the samples		
ζ potential	straightforward method to measure surface charge and changes in surface charge; indicator of stability of NP dispersions	requires a minimum ionic strength and that the NPs be monodisperse as calculates a charge/size ratio	
chromatography	very sensitive and reliable (provided that the method is carried out carefully without any contamination); complex mixtures can be separated accurately using only a few micrograms of sample; separation takes less time as compared to other techniques; the equipment setups are simple and easy	since the method is very sensitive, improper setup or contamination, even in nanograms, will give different results; sample is generally very diluted afterward and requires reconcentration; time consuming	

Table 2. Continued

analytical method	advantages	disadvantages	refs
electrophoresis	suitable for separation of complicated protein mixtures; suitable for qualitative and quantitative analysis	proteins are easily adsorbed onto the inner surface of the capillary, and the detection sensitivity is not high	177, 176
SPR	sensitive to changes in the refractive index of the medium surrounding the sensor and to the thickness of the sensor layer; as any change in protein conformation will bring a modification in this parameter, SPR has also been extensively used to study the conformation of immobilized proteins in various environments	sensitivity of the system with a detection limit restricted to 1–10 nM of a 20 kDa protein and even higher for smaller molecules, particularly when the receptor displays a weak affinity	
QCM	simple, cost-effective, high-resolution mass sensing technique; ease of setup and operation and low cost; QCMs are capable of measuring mass changes as small as a fraction of a monolayer or single layer of atoms; allows a label-free detection of molecules	variations in interfacial parameters, such as surface roughness, surface free energy, surface charge, and viscoelasticity, hamper interpretation of QCM results	

in the last decade it has become a powerful and essential instrument in life science and proteomics studies, where it is used as an high-throughput, analytical tool to identify proteins. The MS analysis process consists of an initial generation of gas-phase analytes from either a crystalline solid form (MALDI, matrix-assisted laser desorption ionization) or a liquid solution (electrospray ionization, ESI). For protein identification purposes, generally a protein sample needs to be first digested into smaller peptides with a proteolytic enzyme (normally trypsin) in order to reduce the size of the analytes and make it more suitable to the useful mass range of the instrument. Peptides are ionized in the ion source and are then introduced into a region of high vacuum. The ions are then separated on the base of their mass to charge ratio (m/z) under either a strong electromagnetic field or in a long drift tube, according to the mass analyzer used. Most of the instruments available on the market perform a so-called tandem or multiple stage (MS n) fragmentation of chosen precursor ions, producing fragments whose size differ from one another by the mass of a constituent amino acid. Upon scanning of the fragments produced, a tandem mass spectrum is obtained, which contains all the information necessary to decipher the primary sequence of each given peptide in the mixture. The raw data are then searched against the database of the species used in the experiment to obtain the protein identities.

There are now several mass spectrometers of different kind available that satisfy any particular need, ensuring high resolution, reduced costs, and small size, although all require a highly trained user to run the instrument.

MS is the technique of choice for protein corona studies as it provides qualitative and quantitative information regarding the protein mixture. It has been successfully applied to identify NP protein coronas using non-gel and gel-based methodologies. The gel-based methodology, which is a classic one, requires previous sample separation on SDS–PAGE. The bands of interest are cut, followed by in-gel trypsin digestion to extract the peptides and analysis by mass spectrometry. The non-gel-based approach requires in-solution trypsin digestion of the proteins while they are still adsorbed on the NP surface. As the proteins are quite compacted on the NP surface, the domains for trypsin digestion may not be accessible, and thus, protein denaturation is necessary. The choice of the denaturing agent has to be made carefully to avoid reduction of trypsin efficacy.^{24,26,137,176,178,189,190,176,179,180,191}

As peptide mixtures can be too complex for a single-run MS analysis, peptides can be separated using 2-D high-performance liquid chromatography (HPLC), generally strong ion exchange followed by reversed-phase chromatography at the interface of the MS.

In both approaches, MS provides qualitative (protein identities) and semi or quantitative values that reflect protein abundance. Quantitative MS can be obtained by pre-labeling the peptide with isotope-coded tags (iTraQ) or in a label free manner that relies on spectral counting and measuring of chromatographic peak areas.²²

5.4.3. Surface Plasmon Resonance. SPR technology is based on the change of oscillation of surface plasmon waves that are caused by the adsorption of molecules onto a metal surface. SPR was used to study the kinetics of NP–protein binding.^{12,44,133} NPs are anchored on the gold surface of the sensor chip, and proteins are injected to flow over the NP-modified surface. Human plasma proteins were injected into the flow chamber and allowed to bind to and release from NIPAM/

BAM copolymer NPs.¹² This confirmed that the more hydrophobic NPs bound more significant amounts of protein and that the association and dissociation rates were clearly dependent on the hydrophobicity of the particles.¹²

5.4.4. Quartz Crystal Microbalance. Quartz crystal microbalance (QCM) is a sensing technology based on the piezoelectric effect. It measures the resonant frequency shift that can be correlated with mass changes at the oscillating quartz surface.^{192,193} Either proteins or NPs are immobilized onto a gold surface on a quartz crystal. The binding partner (NP or protein) is then injected into the flow-chamber and flows over the quartz surface. The frequency is monitored in real time. Real-time and quantitative NP–protein binding profiles are obtained, and the association and dissociation constants can be determined by fitting to the Langmuir adsorption isotherm. The advantages of QCM over SPR are the ease of the setup and operation in addition to low cost and the possibility to use material surfaces other than gold. QCM also allows for multilayer adsorptions (QCM showed no reduction of sensitivity at even 400 nm thickness, whereas SPR showed significant peak broadening at 200 nm thickness). However, the instrumentation and software of SPR are more advanced.^{192,193}

5.5. Advantages and Limitations of the Available Methods

The advantages and limitations of the available methods are summarized in Table 2.

5.6. Request for Possible New Methods

There is tremendous growth in the development of nanomaterials with enhanced performance characteristics. Many “legacy materials” have already found widespread commercial use without a full understanding of their biological reactivity and potential impacts. Although industry desires the safe, widespread use of nanotechnology, it will not occur unless surface characterization and corona identification are possible using simple and accessible laboratory equipment. Static and single-point measurements/single NP–protein measurements are insufficient; the intermediary regimen must accommodate the dynamic and metastable states present at the bio-nano interface in complex biological milieu.²³

Many technologies are emerging that will enable a better understanding of the bio-nano interface, but there is still the need to develop new methodologies to study the interactions between biomolecules and nanoparticles that result in the formation of a protein-modified surface such as occurs when NPs are incubated in human bodily fluids. Additionally, methods to provide detailed descriptions of the biointerface at the NP surface, and how this interacts onward, i.e., with other proteins and cellular receptors, is required. One approach that may help to achieve this is by screening NP–corona complexes against arrays of potential binding targets (e.g., proteins, antibodies) and identifying their binding partners. The great potential of this approach resides in the parallel investigation of multiple biomolecule targets competing for association with the NP surface, thereby mimicking the living medium and hence giving us important information about the interaction pattern and the kinetics aspects of the binding of NP–corona complexes and their subsequent interactions with cell surface receptors. Protein and antibody arrays have been extensively exploited as analytical tools to detect tiny amounts of molecular species in solution and to study the expression of biological functions (biomarker identification), but they have

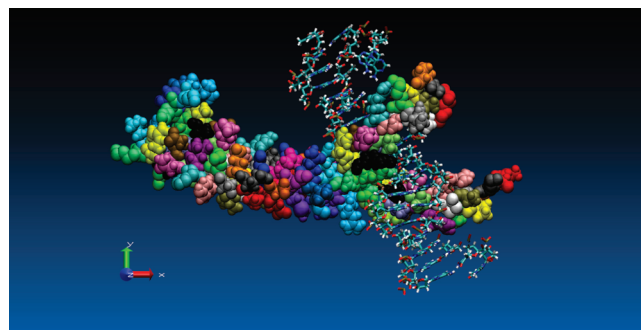


Figure 8. A GCN4 protein binds a DNA at specific sites. The simulation box contains the protein (1728 atoms), DNA segment (1270 atoms), water molecules (38193 molecules), and 61 sodium ions. The picture was taken after relaxation of an NVT (N, number of particles; V, volume; T, temperature) ensemble for about 50 ns at 293 K.

never before been used to “map” the interaction of NPs with biological binders. The rational study of several selected NPs with arrays of binding targets can potentially give new results that will have a high impact in the promising and important fields of nanomedicine and nanotoxicology. By combining protein microarray technology with the use of large human protein expression libraries, we can profile nanoparticle interactions against an almost complete repertoire of human proteins, hopefully identifying key recognition interactions, with major implications for targeted therapy for intractable diseases.

From a more structural point of view, AFM, where a cantilever is vibrated independently at a slightly different frequency, allowing the AFM tip to reveal the accompanying contrast in acoustic impedance as nanoscale heterogeneity, can be used to study the interaction strength between protein-modified NPs and a lipid-supported bilayer (as a model of the cellular membrane).¹⁹⁷ Surface-enhanced Raman scattering (SERS) is being used increasingly for bioimaging of cells. This technique measures the enhanced Raman scattering of molecules adsorbed on metal surfaces. This method is sensitive enough to detect single NPs (PEGylated Au and Ag NPs, for example¹⁹⁷). Recent tumor imaging with radiolabeled single-walled carbon nanotubes (SWCNTs) suggests that SERS may be a promising molecular imaging technique in living subjects.¹⁹⁸ However, such techniques are not routinely available, require skilled workers, and may not be applicable across a broad range of NPs. Ideally, approaches combining chemical mapping and particle sizing in a complex milieu are required to accommodate the broad range of different NPs being developed around the world (estimates place this at being >30000 different NPs).

6. SIMULATION OF NP–PROTEIN INTERACTIONS

Investigation of the dynamics, thermodynamics, and mechanical properties of bio-nano systems at different spatial and temporal resolutions is necessary to understand and control both the applications and the risks of NPs in contact with living systems. In particular, the interaction of nanoparticles with the binding sites/functional units of proteins is very important to understand. As experimental methods to study in detail the interactions and conformational changes of individual nanoparticle–protein conjugates are so limited at present, a natural

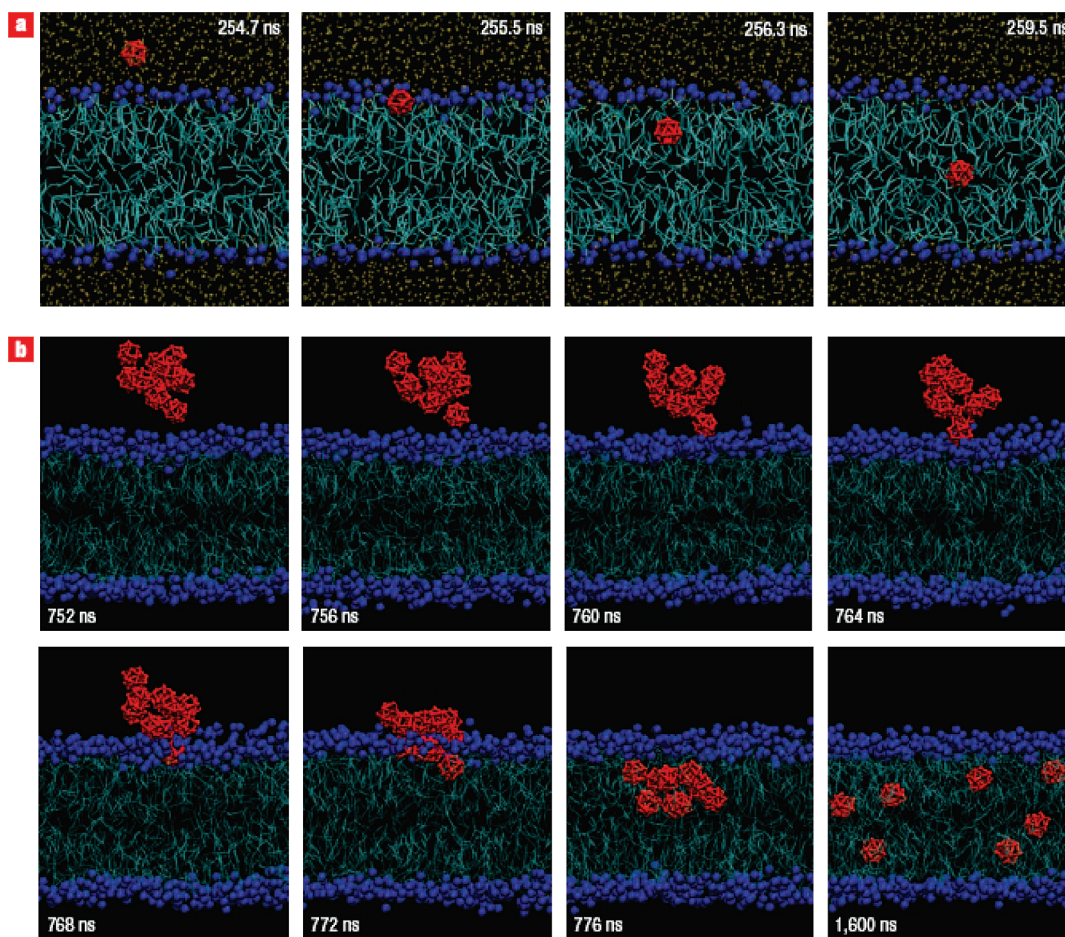


Figure 9. Fullerene permeation through a lipid membrane. A single fullerene is captured in the membrane interior after it escapes quickly from the water environment (a), but the clusters permeate much more slowly (b). Fullerene is shown in red, the lipids are shown in cyan with blue head groups (phosphodiester groups), and water is yellow. Reprinted with permission from ref 209. Copyright 2008 Nature Publishing Group.

alternative is computer simulation. However, at present, such simulations are also limited to single-protein–NP studies, which are not fully representative of the situation in complex biofluids.

NPs and proteins are more complicated than simple hard spheres, which are the typical unit of simulations. In recent years, there have been large efforts dedicated to understanding the structure and the dynamics of these objects by means of different simulation methods.¹⁹⁹ For many crystalline NPs, quantum ab initio methods are relatively successful at providing some information about both the mechanical and electronic structure,^{200,201} although this is not feasible for proteins because of the lack of symmetry of proteins, each of which has a highly controlled, primary, secondary, and tertiary structure, and also as a result of the size of the systems in question. For example, a typical protein with 100 residues in an aquatic medium consists of about 10^5 atoms in a simulation. Figure 8 shows a snapshot of a protein–DNA molecular dynamics (MD) simulation. The figure shows how a GCN4 leucine zipper which is a transcriptional regulator protein recognizes a DNA specific site and binds to it.

Proteins have different residues with different hydrophobicities, and they do not carry a uniform charge. MD is a powerful tool to simulate such systems; however, the goodness of the

results depends greatly on the size of the system and also on the force field parametrization.²⁰² Thus, the most efficient simulation methods for individual NP and protein systems are different, which makes NP–protein simulations even more challenging.

There are numerous nonspecific interactions between NPs and proteins, and the nature of many of them is not yet completely understood. Amino acid side chains may bind to NPs, noncovalently or covalently. NP surfaces are also not perfect; they can have multicrystalline structures with vertices, steps, edges, and defects as well as impurities,²⁰³ and an additional complexity comes from the size distribution of most (all) NP dispersions, as well as the tendency of many nanoparticles to aggregate in biological fluids, thereby altering the available surface area for interaction with proteins. Atoms, sitting at different positions, have different chemical affinities to interact with different protein domains. In many cases, NPs are coated by ligands which act as an interface in NP–protein interactions.^{204,205} Moreover, when nanomaterials are being introduced into biological systems, the water solubility of the particle is also an important issue.

For many systems, simulating all of the NP atoms is computationally very expensive (because of the size of the NP); however, for large enough particles, the details may be washed out. In this way, an extended particle may be presented

Table 3. Comparison of the Appropriate Scales, Advantages, and Weak Points of the Various Simulation Methods

Method	System size	Simulation time	Applicable to	Results	Shortcomings
Quantum Mechanics	First principle ab initio	10 ⁻¹² seconds	Small NPs, ligands	Electronic and mechanical structure; chemical bonds and reactions	Far from relevant biological time and size scales
	Semi-empirical	10 ⁻¹⁰ seconds			
All atom simulations	Molecular Dynamics (MD)	Up to micro seconds	Systems of small proteins and small nanoparticles	Dynamics and thermodynamics, Free energy landscape, rapid transitions,	Still far from many relevant biological time scales, but good to detect local deformations, does not allow bond formation or breaking
	Monte Carlo (MC)			Statistics of equilibrated systems, Free energy landscape	
Coarse Grained	Molecular Dynamics (MD)	Hundreds of micro seconds	Large proteins and NPs, membrane and vesicles	Dynamics, Thermodynamics, diffusion and transportation	Not completely reliable as ignoring much detail
	Monte Carlo (MC)			Conformations, transportation/diffusion	

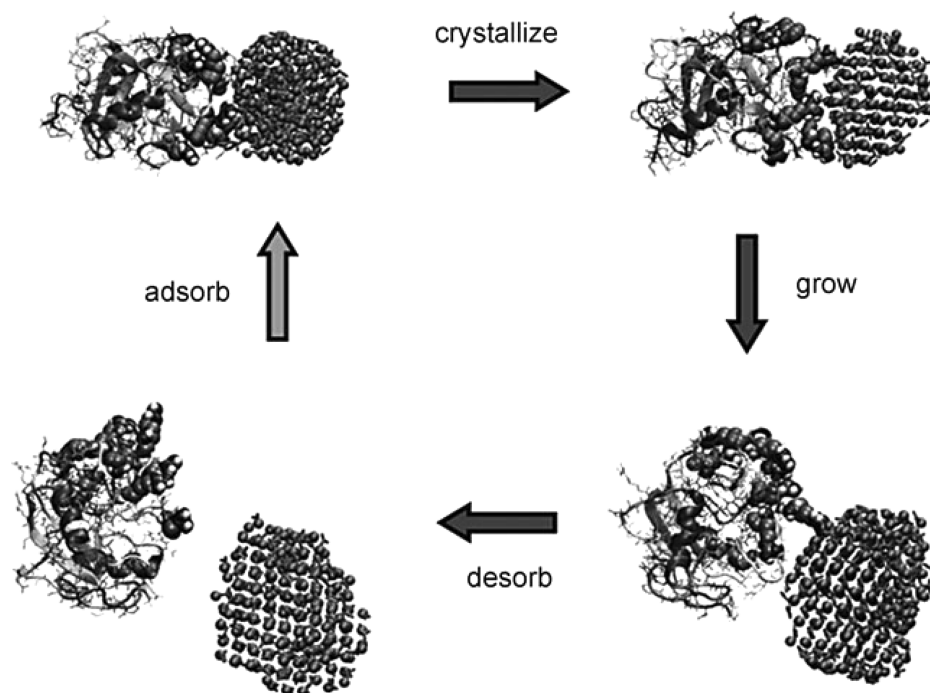


Figure 10. Chicken eggshell ovocleidin-17 protein acts as a catalyst in the transformation of amorphous calcium carbonate to calcite crystals. Reprinted with permission from ref 220. Copyright 2010 Wiley-VCH.

as a surface. For example, it was shown that interaction of yeast cytochrome *c* with hydrophilic surfaces is stronger than with hydrophobic surfaces.²⁰⁶ However, a limit of this approach is that potentially important effects such as those resulting from surface curvature and packing efficiency are diluted or removed. Therefore, this approach is not entirely representative of the true NP–protein interaction, especially for smaller NPs with higher surface curvature where the size of the NP comes close to the size of larger proteins (e.g., fibrinogen and HSA).²⁰⁶

6.1. Simulation Results for NP–Protein Interactions

The adsorption or covalent binding of a protein onto a NP's surface can strongly alter the physio-chemical and structural properties of both of them. It can even unfold the protein. On the other hand, a protein can also change the crystal structure of the NP. To reduce the complexity of the problem, it is usually simplified by considering one of the objects as being unperturbed.

This is a good approximation for highly stable NPs such as fullerenes or carbon nanotubes (CNTs). Energetically favorable binding modes between antibodies and fullerene have been identified both in MD²⁰⁷ and in combined MD–docking studies.²⁰⁸ The thermodynamics and mechanism of permeation of fullerene aggregates (Figure 9)²⁰⁹ and CNTs through cell membranes^{210,211} and also water molecule transport through carbon nanotubes²¹² have been described where the NPs are considered as being rigid or coarse-grained (CG). In comparison to more detailed atomistic models, CG models make simulations feasible at longer time and/or length scales.²¹³ The appropriate scales, advantages, and disadvantages of the different simulation methods are compared in Table 3.

There are also other ways to accelerate atomistic simulations. If the question is related to equilibrium states or transition

pathways between protein folding states, the topology of the free energy landscape²¹⁴ or its projections on some given reaction coordinates may have enough information to help understand the system. This can be performed using methods such as Monte Carlo (MC), Brownian dynamics, metadynamics, or umbrella sampling.^{215,216} Metadynamics samples the free energy landscape and projects it onto a subspace of a few reaction coordinates to find transition pathways between different states and could potentially be used to assess conformation changes of proteins upon binding to NPs. The method shows good performance for modeling the clustering of inorganic ions on biomolecules.²¹⁷ The contribution of native proteins to crystal nucleation of mineral NPs has been reported experimentally,^{218,219} but the time scale is not accessible to ordinary atomistic molecular dynamic simulations. It has been shown that the process can be investigated using metadynamics,²²⁰ where the results propose that chicken eggshell protein ovocleidin-17 acts as a catalyst by binding to CaCO_3 NPs, causing crystal nucleation, and then leaves it to grow (Figure 10).

One particular issue in NP–protein interactions is conjugation, where proteins are covalently linked to the NP. This can affect both the structure and function of the protein, and typically several different protein orientations are observed.³⁷ Despite these complications, the model usually oversimplifies the situation, and proteins are often assumed to be fully folded, which may cause the loss of relevant information for physics and biology.²²¹

For covalently linked proteins, it is shown that linkage can affect the charge distribution of the ligands and the overall charge of the NPs. MD simulations show that even labeling sites may affect the protein conformation and would contribute (e.g. labelling of the proteins might itself affect the protein

conformation and thus its binding to NPs).²²¹ As an example, in labeling cytochrome *c* by Au NPs, there are key motifs on the protein that induce local denaturation if they are labeled. Simulations propose that in order to preserve protein structure, flexible and loosely folded motifs should be labeled instead of folding nucleation centers.²²¹

First-principle calculations, which are widely used for investigation of subatomic detailed structure of nanoscaled systems,²²² can be applied to tiny systems of NP–biomaterials. A good example is the interaction of DNA base pairs with the outer surface of CNTs,²²³ which can be studied by the application of density functional theory (DFT).²²⁴ In addition to reporting on the protein structure, such ab initio quantum calculations are able to find charge density and may help to realize the nature of the chemical forces driving the interactions.²²⁴

6.2. NP Self-Assembly

DNA sequences can be attached to gold NP to form novel DNA–NP assemblies.²²⁵ The known DNA oligonucleotides are chemically attached to metallic NPs (mostly Au) to create DNA probes with the capability to self-assemble into aggregates.²²⁶ The particles interact with each other through base-pairing. The base-pair interactions make the assembly programmable as the nature of the interactions (DNA melting and hybridization) makes it tunable and controllable.^{225,227}

Parameters such as temperature or concentration not only can control transitions in the system, but may also enable the particles to self-assemble into preprogrammed structures. Although the length and time scales of the systems do not allow detailed atomistic simulations, there are successful efforts to investigate the interesting physics of the system by means of coarse-grained MC or MD simulation.^{228,229}

6.3. NPs in Larger Biological Systems

As mentioned previously, NPs may be harmful when adsorbed to the membrane of living cells in cases where such interactions were not intended. Thus, the interaction of NPs with the membrane has attracted huge interest in recent years.²³⁰

By means of Brownian dynamic simulations, it has been shown that adhesive NPs induce morphological change of the vesicle membrane.²³¹ Spherical NPs, which interact with the hydrophilic part of the bilayer, induce wrapping of the membrane around the NP, and formation of pore openings was observed during the simulation.²³¹

In a more detailed atomistic MD simulation, interaction between a carbonaceous NP and a pulmonary surfactant monolayer has been investigated.²³² Here also, the lipid membrane wrapped around the NP during the simulation.

7. OUTCOME OF PROTEIN–NP INTERACTIONS

Although NPs have significant potential for use in many medical applications, there are also potential “toxic” phenomena that are observed^{233–237} (overexpression of inflammatory factors,^{238,239} production of reactive oxygen species,^{82,240,241} uncontrolled aggregation or amyloidosis diseases²⁴²) and whose biological and physiological implications must be understood. NPs possess large surface/volume ratios (for example, there are 800 m² of surface area per liter of 1 wt % dispersion of 70 nm particles).⁴⁴ In a physiological medium, NPs are coated with proteins whose conformation may be disrupted or

induced to aggregate, which can trigger unexpected cellular responses.¹⁰⁴ The adsorbed proteins are similar enough to the native protein that the cells do not recognize them as denatured, but may be sufficiently different from the native form that they trigger an inappropriate cellular process. Linse et al.⁴⁴ reported that NPs enhance the probability of appearance of a critical nucleus for nucleation of protein fibrils from human b2-microglobulin in solution. These phenomena increase the risk of toxic clusters and amyloid formation, although whether this also occurs under competitive binding conditions has not yet been shown.

Kreuter et al.²⁴³ showed that (i) transport across the blood–brain barrier was initiated by surface-bound apolipoproteins, which can be taken up by brain capillary endothelial cells, and (ii) the antinociceptive effect of the enkephalin analogue dalargin was significantly enhanced when loaded into apolipoprotein-coated NPs. A recent study using iron oxide NPs modified with chlorotoxin to image brain tumors showed transport across the blood–brain barrier for excellent tumor imaging.²⁴⁴ However, the mechanism of transport was not clear. It is possible that circulating apolipoproteins may have contributed to the uptake of these NPs. These studies are examples of using serum protein binding as an advantage. However, the protein corona surrounding the NP is often uncontrolled and thus not beneficial for targeting because it can lead to accumulation in the reticuloendothelial system.²⁴⁵

8. WHAT NEXT?

The developments in nanotechnology are leading to potential applications in multiple areas, such as in composites, coatings, electronics, information technology, and more recently health care and the life sciences. Due to its rapid propagation into all branches of science, the current century may have cause to be named the “Nanotechnology Age”. The number of publications in the field of nanotechnology has increased rapidly in recent years; however, the majority of these investigations are focused on the synthesis, characterization, and surface properties of NPs, whereas the biological issues have been the subject of less attention. Due to the importance of the potential toxicity of NPs and the need to ensure the safe implementation of nanotechnologies, their biological behaviors are currently recognized as a crucial issue that needs to be addressed urgently.^{13,23} As described in this paper, the biological impacts of NPs are mostly related to, and determined by, the modified surface of NPs following interaction with biological molecules (i.e., by the formation of a protein corona), rather than by the composition or characteristics of the original surface of the NP itself.

Early work published in 2007 brought attention to the biological impact of the formation of a protein corona on the surface of NPs and on its huge importance for the safe use of NPs for biomedical applications. This is now a well-established phenomenon which is carefully considered by most researchers in this field.^{27,30,46,49,55–58,87,246}

According to human experience throughout history, the contribution of every new research endeavor to human science can be truly judged only once the dust settles.²⁴⁷ To date, while the scientific findings pertaining to the NP–protein corona and its consequent biological impacts are becoming relatively well established, much more work is needed to really understand and

predict biological impacts based on the composition of the NP–protein corona. Therefore, it is not yet time to evaluate the significance of the technological promises and the future perspectives of this matter.

Besides those NPs which are directly used for biomedical applications and which are now available as commercial products, there are many other products that contain NPs, such as sunscreens, which consist of several metal oxide NPs.⁸⁷ People and more specifically certain occupational groups (e.g., welders and workers in steel mills) may be directly exposed to various types of NPs.⁸⁷ Hence, a deep understanding of the potential side effects of NPs must be achieved to prevent any negative health implications from nanotechnology in the future.²⁴⁸ Therefore, without the appropriate biological and physiological data and consequently the removal of uncertainty regarding the implications of nanotechnology, the famous sentence of Richard Feynman that “There’s plenty of room at the bottom” (which was the first hint of the emergence of nanotechnology) may be changed to “There’s a few safe NPs at the bottom!” (which will indicate those NPs that have been shown beyond doubt to be safe for use in medicine and diagnostics). Nanomaterials have generated tremendous interest due to the fact that they present an opportunity to deliver unprecedented material performance. These opportunities are based on the unique properties (e.g., magnetic, optical, mechanical, electronic) that vary continuously or abruptly with changes in the size of the material at the nanoscale. These steplike changes in nanoscale properties provide both enormous potential and challenges. Globally, these breakthroughs will enable key advances in health care, such as targeted drug delivery, diagnostics, and biosensors.

Nanomaterials designed from the “bottom up” will deliver the specific combination of functions needed for their application. Material developers of the future will identify the optimal material properties for each application and select the appropriate building blocks and production technology to efficiently and economically produce the material with the desired properties and function.

Revolutionary advances in science and technology enable the solution-oriented design of nanomaterials. In-depth understanding of physics and chemistry fundamentals at the nanoscale, combined with modern, robust, computational capability across length scales, also enables the directed design and synthesis of libraries of high-quality nanomaterial building blocks. Understanding of the fundamentals will assist in the development of models and tools and help to verify the accuracy of that understanding. Knowledge of the relationships among structure, properties, functions, and processing methods will provide the basis for application-based protein–nanoparticle design.

Systems which have integrated imaging, spectroscopy, and scattering capabilities to provide the array of information necessary to characterize nanomaterial features and behavior across relevant scales should be developed. Development of these capabilities will evolve in steps, starting from an instantaneous measurement of a single property at multiple nanoscale locations, moving to multiple properties at a single nanoscale location, and finally to generating a real-time, 3-D map of both chemical and physical properties. Ultimately, this tool will need to meet the requirements of a demanding range of life science and technology studies.

9. CONCLUSIONS

The emerging fields of nanoscience and nanoengineering are leading to unprecedented understanding and control over the fundamental building blocks of all physical things. Nanoscience will provide tremendous potential for biomedical research and application. The key role of protein–nanoparticle interactions in nanomedicine and nanotoxicity has begun to emerge recently via the identification of the NP–protein (biomolecule) corona. This dynamic layer of proteins and/or other biomolecules adsorbed to the nanoparticle surface determines how a NP interacts with living systems and thereby modifies the cellular responses to the NPs.

We have shown here a range of different parameters which affect protein adsorption and subsequent cellular responses to NPs and also the methods used for characterizations of the nanoparticle–protein “corona”. On this basis, we have shown that there is significant new potential for understanding nanoparticle–protein interactions and thereby to influence cellular behavior and response to NPs. In particular, there is considerable scope for nanomaterial “safety by design” via tailoring of the NPs’ physicochemical properties to predetermine the nature and conformation of the proteins that adsorb, to acquire a specific, desired biological identity via the protein (biomolecule) corona.

AUTHOR INFORMATION

Corresponding Author

*E-mail: mahmoudi@biospion.com.

BIOGRAPHIES



Dr. Morteza Mahmoudi obtained his Ph.D. in 2009 from the Sharif University of Technology with specialization in the cytotoxicity of superparamagnetic iron oxide nanoparticles (SPIONs). He has received many awards, such as the Shahid Chamran Award (National Endowment for the Elite, 2011), Distinguished Researcher at Pasteur Institute of Iran (2010), the Dr. Mojtahedi Innovation Award for Distinguished Innovation in Research and Education at Sharif University of Technology (2010), and the Kharazmi Young Festival Award (2009). His current research involves the magic SPION for simultaneous diagnosis and therapeutic applications (<http://www.biospion.com>). He is the author of the book entitled *Superparamagnetic Iron Oxide Nanoparticles for Biomedical Applications*, which is published by Nova Science Publishers, New York. He was a visiting scientist at the Laboratory of

Powder Technology (LTP) and Center for BioNano Interactions (CBNI) at the Swiss Federal Institute of Technology (EPFL) and University College of Dublin (UCD) under the supervision of Professor Heinrich Hofmann and Professor Kenneth A. Dawson, respectively.



Dr. Iseult Lynch is the Strategic Research Manager for the Centre for BioNano Interactions at the University College of Dublin. She has a Ph.D. in physical chemistry from University College Dublin and did several years of postdoctoral research at Physical Chemistry 1, Lund University, Sweden, as an EU Marie Curie Fellow. She is specialist in synthesis and characterization of nanoparticles and materials for use in biological applications (where cells are sensitive to even nanomolar traces of impurities). Her research work involves the development of novel materials and structures for nanobiology and the detailed physical and biological characterization of these materials. She was part of the team that won the Cozzarelli prize in 2007 from the Proceedings of the US National Academy of Sciences for describing the nanoparticle-protein corona.



Dr. Mohammad Reza Ejtehadi obtained his Ph.D. in physics from the Sharif University of Technology, Tehran, in 1998. He has worked at the Max-Planck Institute for Polymer Research in Mainz and the University of British Columbia in Vancouver, and in 2004 he joined the Sharif University of Technology, where he has held an associate professor position since 2008. He applies statistical physics and simulation to various problems in soft matter and biological systems. He was also elected a board member of the Physics Society of Iran in 2009.



Marco P. Monopoli graduated from the Università degli studi di Modena e Reggio Emilia in Biotecnologie Farmaceutiche in 2005 and started his Ph.D. in the Applied Neurotherapeutics Research Group at the Conway Institute, University College of Dublin, where he investigated protein associate changes using a large study in proteomics. During his Ph.D. studies, he worked closely with Professor Micheal J. Dunn and Stephen Pennington and become familiar with 2-D gel electrophoresis and mass spectrometry. In 2008 he joined the Centre for BioNano Interactions at the University College of Dublin, where he is studying protein association with nanoparticles of different charges, sizes, and materials.



Dr. Francesca Baldelli Bombelli is a Lecturer in Colloid Science and Nanotechnology at the University of East Anglia where she has just started her own group. Before that, she has worked as PostDoctoral Fellow at the Centre for BioNano Interactions for two years where her research is aimed at developing a new methodology for studying the interactions between selected biomolecules and meso-nanoparticle-protein complexes obtained in biological fluids. Francesca received her doctoral degree in chemical science in 2004 at the University of Florence, Florence, Italy, where she studied self-assembly properties of nucleolipids to control the relationships between the molecular structure of different nucleolipids and the self-aggregation behavior at the mesoscale. After that, she was awarded a postdoctoral fellowship from the University of Florence and worked within an FP6 European Project (AMNA) aimed to develop nanoscale-functionalized surfaces based on a digitally addressable DNA molecular grid. During this postdoctoral period she worked for a year at the Department of

Chemistry and Bioscience at Chalmers University, Gothenburg, Sweden.



Dr. Sophie Laurent was born in 1967. Her studies were performed at the University of Mons-Hainaut, Belgium, where she received her Ph.D. in chemistry in 1993. She then joined Professor R. N. Muller's team and was involved in the development (synthesis and physicochemical characterization) of paramagnetic Gd complexes and superparamagnetic iron oxide nanoparticles as contrast agents for magnetic resonance imaging. She is currently working on the vectorization of contrast agents for molecular imaging. She is a lecturer and coauthor of around 90 publications and more than 180 communications at international meetings.

ACKNOWLEDGMENT

We thank Mr. Meisam Rezaei from the Sharif University of Technology for his constructive comments on the simulation part. We also thank Dr. Ben Wang from the Harvard Medical School for his helpful notes on Table 2.

REFERENCES

- (1) Nirmal, M.; Brus, L. *Acc. Chem. Res.* **1999**, *32*, 407.
- (2) Alivisatos, A. P. *Science* **1996**, *271*, 933.
- (3) Chan, W. C. W.; Nie, S. *Science* **1998**, *281*, 2016.
- (4) Dujardin, E.; Mann, S. *Adv. Mater.* **2002**, *11*, 775.
- (5) Wang, Y. *Acc. Chem. Res.* **1991**, *24*, 133.
- (6) Steigerwald, M. L.; Brus, L. E. *Acc. Chem. Res.* **1990**, *23*, 183.
- (7) Weller, H. *Adv. Mater.* **1993**, *5*, 88.
- (8) Mahmoudi, M.; Sahraian, M. A.; Shokrgozar, M. A.; Laurent, S. *ACS Chem. Neurosci.* **2011**, *2*, 118.
- (9) Nic Ragnair, M.; Brown, M.; Ye, D.; Bramini, M.; Callanan, S.; Lynch, I.; Dawson, K. A. *Eur. J. Pharm. Biopharm.* **2011**, *77*, 360.
- (10) Mahmoudi, M.; Azadmanesh, K.; Shokrgozar, M. A.; Journeay, W. S.; Laurent, S. *Chem. Rev.* **2011**, *111*, 3407.
- (11) Fadeel, B.; Garcia-Bennett, A. E. *Adv. Drug Delivery Rev.* **2010**, *62*, 362.
- (12) Cedervall, T.; Lynch, I.; Lindman, S.; Berggard, T.; Thulin, E.; Nilsson, H.; Dawson, K. A.; Linse, S. *Proc. Natl. Acad. Sci. U.S.A.* **2007**, *104*, 2050.
- (13) Mahmoudi, M.; Sant, S.; Wang, B.; Laurent, S.; Sen, T. *Adv. Drug Delivery Rev.* **2011**, *63*, 24.
- (14) Norde, W.; Gags, D. *Langmuir* **2004**, *20*, 4162.
- (15) Gray, J. J. *Curr. Opin. Struct. Biol.* **2004**, *14*, 110.
- (16) Wilson, C. J.; Clegg, R. E.; Leavesley, D. I.; Percy, M. J. *Tissue Eng.* **2005**, *11*, 1.
- (17) Engel, M. F. M.; Visser, A. J. W. G.; Van Mierlo, C. P. M. *Proc. Natl. Acad. Sci. U.S.A.* **2004**, *101*, 11316.
- (18) Shen, M.; Garcia, I.; Maier, R. V.; Horbett, T. A. *J. Biomed. Mater. Res., Part A* **2004**, *70*, 533.
- (19) Norde, W.; Lyklema, J. *J. Biomater. Sci., Polym. Ed.* **1991**, *2*, 183.
- (20) Lynch, I.; Dawson, K. A. *Nano Today* **2008**, *3*, 40.
- (21) Klein, J. *Proc. Natl. Acad. Sci. U.S.A.* **2007**, *104*, 2029.
- (22) Monopoli, M. P.; Walczyk, D.; Lowry-Campbell, A.; Elia, G.; Lynch, I.; B.F., B.; Dawson, K. A. *J. Am. Chem. Soc.* **2011**, *133*, 2525.
- (23) Nel, A. E.; Madler, L.; Velegol, D.; Xia, T.; Hoek, E. M. V.; Somasundaran, P.; Klaessig, F.; Castranova, V.; Thompson, M. *Nat. Mater.* **2009**, *8*, 543.
- (24) Cedervall, T.; Lynch, I.; Foy, M.; Berggard, T.; Donnelly, S. C.; Cagney, G.; Linse, S.; Dawson, K. A. *Angew. Chem., Int. Ed.* **2007**, *46*, 5754.
- (25) Lindman, S.; Lynch, I.; Thulin, E.; Nilsson, H.; Dawson, K. A.; Linse, S. *Nano Lett.* **2007**, *7*, 914.
- (26) Lundqvist, M.; Stigler, J.; Elia, G.; Lynch, I.; Cedervall, T.; Dawson, K. A. *Proc. Natl. Acad. Sci. U.S.A.* **2008**, *105*, 14265.
- (27) Mahmoudi, M.; Simchi, A.; Imani, M. *J. Iran. Chem. Soc.* **2010**, *7*, S1.
- (28) Mahmoudi, M.; Milani, A. S.; Stroeve, P. *Int. J. Biomed. Nanosci. Nanotechnol.* **2010**, *1*, 164.
- (29) Watson, P.; Jones, A. T.; Stephens, D. J. *Adv. Drug Delivery Rev.* **2005**, *57*, 43.
- (30) Mahmoudi, M.; Simchi, A.; Imani, M. *J. Phys. Chem. C* **2009**, *113*, 9573.
- (31) Jiang, W.; Kim, B. Y. S.; Rutka, J. T.; Chan, W. C. W. *Nat. Nanotechnol.* **2008**, *3*, 145.
- (32) Gratton, S. E. A.; Ropp, P. A.; Pohlhaus, P. D.; Luft, J. C.; Madden, V. J.; Napier, M. E.; DeSimone, J. M. *Proc. Natl. Acad. Sci. U.S.A.* **2008**, *105*, 11613.
- (33) Chithrani, B. D.; Chan, W. C. W. *Nano Lett.* **2007**, *7*, 1542.
- (34) De Paoli Lacerda, S. H.; Park, J. J.; Meuse, C.; Pristinski, D.; Becker, M. L.; Karim, A.; Douglas, J. F. *ACS Nano* **2010**, *4*, 365.
- (35) Mahmoudi, M.; Sardari, S.; Shokrgozar, M. A.; Laurent, S.; Stroeve, P. *Nanoscale* **2011**, *3*, 1127.
- (36) Rezwani, K.; Studart, A. R.; Vörös, J.; Gauckler, L. J. *J. Phys. Chem. B* **2005**, *109*, 14469.
- (37) Aubin-Tam, M. E.; Hamad-Schifferli, K. *Biomed. Mater.* **2008**, *3*, 034001.
- (38) Vauthier, C.; Lindner, P.; Cabane, B. *Colloids Surf., B* **2009**, *69*, 207.
- (39) Koo, E. H.; P.T., L.; Kelly, J. W. *Proc. Natl. Acad. Sci. U.S.A.* **1999**, *96*, 9989.
- (40) Huff, M. E.; Balch, W. E.; Kelly, J. W. *Curr. Opin. Struct. Biol.* **2003**, *13*, 674.
- (41) Chiti, F.; Dobson, C. M. *Annu. Rev. Biochem.* **2006**, *75*, 333.
- (42) Dawson, K. A. *Curr. Opin. Colloid Interface Sci.* **2002**, *7*, 218.
- (43) Stradner, A.; Sedgwick, H.; Cardinaux, F.; Poon, W. C. K.; Egelhaaf, S. U.; Schurtenberger, P. *Nature* **2004**, *432*, 492.
- (44) Linse, S.; Cabaleiro-Lago, C.; Xue, W. F.; Lynch, I.; Lindman, S.; Thulin, E.; Radford, S. E.; Dawson, K. A. *Proc. Natl. Acad. Sci. U.S.A.* **2007**, *104*, 8691.
- (45) Ehrenberg, M. S.; Friedman, A. E.; Finkelstein, J. N.; Oberdorster, G.; McGrath, J. L. *Biomaterials* **2009**, *30*, 603.
- (46) Mahmoudi, M.; Shokrgozar, M. A.; Simchi, A.; Imani, M.; Milani, A. S.; Stroeve, P.; Vali, H.; Hafeli, U. O.; Bonakdar, S. *J. Phys. Chem. C* **2009**, *113*, 2322.
- (47) Nemmar, A.; Hoet, P. H. M.; Vanquickenborne, B.; Dinsdale, D.; Thomeer, M.; Hoylaerts, M. F.; Vanbilloen, H.; Mortelmans, L.; Nemery, B. *Circulation* **2002**, *105*, 411.
- (48) Walczyk, D.; Bombelli, F. B.; Monopoli, M. P.; Lynch, I.; Dawson, K. A. *J. Am. Chem. Soc.* **2010**, *132*, 5761.
- (49) Mahmoudi, M.; Simchi, A.; Imani, M.; Shokrgozar, M. A.; Milani, A. S.; Hafeli, U. O.; Stroeve, P. *Colloids Surf., B* **2010**, *75*, 300.
- (50) Harishchandra, R. K.; Saleem, M.; Galla, H. J. *J. R. Soc. Interface* **2010**, *7*, S15.
- (51) Allemann, E.; Gravel, P.; Leroux, J. C.; Balant, L.; Gurny, R. *J. Biomed. Mater. Res., Part A* **1997**, *37*, 229.

- (52) Luck, M.; Paulke, B. R.; Schroder, W.; Blunk, T.; Muller, R. H. *J. Biomed. Mater. Res., Part A* **1998**, *39*, 478.
- (53) Blunk, T.; Hochstrasser, D. F.; Sanchez, J. C.; Muller, B. W.; Muller, R. H. *Electrophoresis* **1993**, *14*, 1382.
- (54) Gessner, A.; Lieske, A.; Paulke, B. R.; Muller, R. H. *J. Biomed. Mater. Res., Part A* **2003**, *65*, 319.
- (55) Mahmoudi, M.; Simchi, A.; Imani, M.; Hafeli, U. O. *J. Phys. Chem. C* **2009**, *113*, 8124.
- (56) Mahmoudi, M.; Simchi, A.; Imani, M.; Milani, A. S.; Stroeve, P. *J. Phys. Chem. B* **2008**, *112*, 14470.
- (57) Mahmoudi, M.; Simchi, A.; Imani, M.; Milani, A. S.; Stroeve, P. *Nanotechnology* **2009**, *20*, 225104.
- (58) Mahmoudi, M.; Simchi, A.; Imani, M.; Stroeve, P.; Sohrabi, A. *Thin Solid Films* **2010**, *518*, 4281.
- (59) Mahmoudi, M.; Simchi, A.; Milani, A. S.; Stroeve, P. *J. Colloid Interface Sci.* **2009**, *336*, 510.
- (60) Mahmoudi, M.; Simchi, A.; Vali, H.; Imani, M.; Shokrgozar, M. A.; Azadmanesh, K.; Azari, F. *Adv. Eng. Mater.* **2009**, *11*, B243.
- (61) Lu, C. F.; Nadarajah, A.; Chittur, K. K. *J. Colloid Interface Sci.* **1994**, *168*, 152.
- (62) Gessner, A.; Lieske, A.; Paulke, B. R.; Muller, R. H. *Eur. J. Pharm. Biopharm.* **2001**, *54*, 165.
- (63) Ehrenberg, M.; McGrath, J. L. *Acta Biomater.* **2005**, *1*, 305.
- (64) Zhang, J.; Badugu, R.; Lakowicz, J. R. *Plasmonics* **2008**, *3*, 3.
- (65) Roach, P.; Farrar, D.; Perry, C. C. *J. Am. Chem. Soc.* **2005**, *127*, 8168.
- (66) Xiao, Q.; Huang, S.; Qi, Z.-D.; Zhou, B.; He, Z.-K.; Liu, Y. *Biochim. Biophys. Acta, Proteins Proteomics* **2008**, *1784*, 1020.
- (67) Brewer, S. H.; Glomm, W. R.; Johnson, M. C.; Knag, M. K.; Franzen, S. *Langmuir* **2005**, *21*, 9303.
- (68) Gao, D.; Tian, Y.; Bi, S.; Chen, Y.; Yu, A.; Zhang, H. *Spectrochim. Acta, Part A* **2005**, *62*, 1203.
- (69) Lundqvist, M.; Sethson, I.; Jonsson, B.-H. *Langmuir* **2004**, *20*, 10639.
- (70) Jennings, T. L.; Singh, M. P.; Strouse, G. F. *J. Am. Chem. Soc.* **2006**, *128*, 5462.
- (71) Cox, M. C.; Barnham, K. J.; Frenkiel, T. A.; Hoeschele, J. D.; Mason, A. B.; He, Q. Y.; Woodworth, R. C.; Sadler, P. J. *J. Biol. Inorg. Chem.* **1999**, *4*, 621.
- (72) Schulze, C.; Kroll, A.; Lehr, C. M.; Schaefer, U. F.; Becker, K.; Schneckeburger, J.; Schulze, C.; Landsiedel, R.; Wohlleben, W. *Nanotoxicology* **2008**, *2*, 51.
- (73) Näreoja, T.; Määttä, A.; Peltonen, J.; Hänninen, P. E.; Härmä, H. *J. Immunol. Methods* **2009**, *347*, 24.
- (74) Näreoja, T.; Vehniäinen, M.; Lamminmäki, U.; Hänninen, P. E.; Härmä, H. *J. Immunol. Methods* **2009**, *345*, 80.
- (75) Jalilian, A. R.; Panahifard, A.; Mahmoudi, M.; Akhlaghi, M.; Simchi, A. *Radiochim. Acta* **2009**, *97*, 51.
- (76) Temming, K.; Lacombe, M.; Van Der Hoeven, P.; Prakash, J.; Gonzalo, T.; Dijkers, E. C. F.; Orfi, L.; Keri, G.; Poelstra, K.; Molema, G.; Kok, R. J. *Bioconjugate Chem.* **2006**, *17*, 1246.
- (77) Gonzalo, T.; Talman, E. G.; Van De Ven, A.; Temming, K.; Greupink, R.; Beljaars, L.; Reker-Smit, C.; Meijer, D. K. F.; Molema, G.; Poelstra, K.; Kok, R. J. *J. Controlled Release* **2006**, *111*, 193.
- (78) Verel, I.; Visser, G. W. M.; Boerman, O. C.; Van Eerd, J. E. M.; Finn, R.; Boellaard, R.; Vosjan, M. J. W. D.; Stigter-Van Walsum, M.; Snow, G. B.; Van Dongen, G. A. M. S. *Cancer Biother. Radiopharm.* **2003**, *18*, 655.
- (79) Jalilian, A. R.; Hosseini-Salekdeh, S. L.; Mahmoudi, M.; Yousefina, H.; Majdabadi, A.; Pouladian, M. *J. Radioanal. Nucl. Chem.* **2011**, *287*, 119.
- (80) Hoek, E. M.; Agarwal, G. K. *J. Colloid Interface Sci.* **2006**, *298*, 50.
- (81) Aitken, R. J.; Chaudhry, M. Q.; Boxall, A. B. A.; Hull, M. *Occup. Med.* **2006**, *56*, 300.
- (82) Xia, T.; Kovichich, M.; Brant, J.; Hotze, M.; Sempff, J.; Oberley, T.; Sioutas, C.; Nel, A. E. *Nano Lett.* **2006**, *6*, 1794.
- (83) Rahman, Q.; Lohani, M.; Dopp, E.; Pemsel, H.; Jonas, L.; Weiss, D. G.; Schiffmann, D. *Environ. Health Perspect.* **2002**, *110*, 797.
- (84) Veranth, J. M.; Kaser, E. G.; Veranth, M. M.; Koch, M.; Yost, G. S. *Part. Fibre Toxicol.* **2007**, *4*, 2.
- (85) Hussain, S. M.; Hess, K. L.; Gearhart, J. M.; Geiss, K. T.; Schlager, J. J. *Toxicol. Vitro* **2005**, *19*, 975.
- (86) Vertegel, A. A.; Siegel, R. W.; Dordick, J. S. *Langmuir* **2004**, *20*, 6800.
- (87) Karlsson, H. L.; Cronholm, P.; Gustafsson, J.; Muller, L. *Chem. Res. Toxicol.* **2008**, *21*, 1726.
- (88) Sousa, S. R.; Moradas-Ferreira, P.; Barbosa, M. A. *J. Mater. Sci.: Mater. Med.* **2005**, *16*, 1173.
- (89) Ellingsen, J. E. *Biomaterials* **1991**, *12*, 593.
- (90) Rezwan, K.; Meier, L. P.; Rezwan, M.; Vörös, J.; Textor, M.; Gauckler, L. J. *Langmuir* **2004**, *20*, 10055.
- (91) Horie, M.; Nishio, K.; Fujita, K.; Endoh, S.; Miyauchi, A.; Saito, Y.; Iwahashi, H.; Yamamoto, K.; Murayama, H.; Nakano, H.; Nanashima, N.; Niki, E.; Yoshida, Y. *Chem. Res. Toxicol.* **2009**, *22*, 543.
- (92) Hughes Wassell, D. T.; Embury, G. *Biomaterials* **1996**, *17*, 859.
- (93) Oliva, F. Y.; Avallé, L. B.; Cámara, O. R.; De Pauli, C. P. *J. Colloid Interface Sci.* **2003**, *261*, 299.
- (94) Kasemo, B. *J. Prosthet. Dent.* **1983**, *49*, 832.
- (95) Klinger, A.; Steinberg, D.; Kohavi, D.; Sela, M. N. *J. Biomed. Mater. Res., Part A* **1997**, *36*, 387.
- (96) Lee, W. A.; Pernodet, N.; Li, B.; Lin, C. H.; Hatchwell, E.; Rafailovich, M. H. *Chem. Commun.* **2007**, *45*, 4815.
- (97) Vevers, W. F.; Jha, A. N. *Ecotoxicology* **2008**, *17*, 410.
- (98) Buijs, J.; Vera, C. C.; Ayala, E.; Steensma, E.; Håkansson, P.; Oscarsson, S. *Anal. Chem.* **1999**, *71*, 3219.
- (99) Kondo, A.; Oku, S.; Murakami, F.; Higashitani, K. *Colloids Surf., B* **1993**, *1*, 197.
- (100) Yu, C. H.; Al-Saadi, A.; Shih, S. J.; Qiu, L.; Tam, K. Y.; Tsang, S. C. *J. Phys. Chem. C* **2009**, *113*, 537.
- (101) Larsericsdotter, H.; Oscarsson, S.; Buijs, J. *J. Colloid Interface Sci.* **2001**, *231*, 98.
- (102) Ehrenberg, M. S.; Friedman, A. E.; Finkelstein, J. N.; Oberdörster, G.; McGrath, J. L. *Biomaterials* **2009**, *30*, 603.
- (103) Chanteau, B.; Fresnais, J.; Berret, J. F. *Langmuir* **2009**, *25*, 9064.
- (104) Lynch, I.; Dawson, K. A.; Linse, S. *Sci. STKE* **2006**, *327*, 14.
- (105) Dawson, K. A.; Salvati, A.; Lynch, I. *Nat. Nanotechnol.* **2009**, *4*, 84.
- (106) Faunce, T. A.; White, J.; Mattheaei, K. I. *Nanomedicine* **2008**, *3*, 859.
- (107) Röcker, C.; Pötzl, M.; Zhang, F.; Parak, W. J.; Nienhaus, G. U. *Nat. Nanotechnol.* **2009**, *49*, 577.
- (108) Shang, L.; Wang, Y.; Jiang, J.; Dong, S. *Langmuir* **2007**, *23*, 2714.
- (109) Dell'Orco, D.; Lundqvist, M.; Oslakovic, C.; Cedervall, T.; Linse, S. *PLoS ONE* **2010**, *5*, e10949.
- (110) Yokoyama, K.; Cho, H.; Cullen, S. P.; Kowalik, M.; Briglio, N. M.; Hoops, H. J.; Zhao, Z.; Carpenter, M. A. *Int. J. Mol. Sci.* **2009**, *10*, 2348.
- (111) Makey, D. G.; Seal, U. S. *Biochim. Biophys. Acta* **1976**, *453*, 250.
- (112) Aisen, P. *Inorganic Chemistry*; Elsevier: New York, 1973; Chapter 9.
- (113) Anderson, B. F.; Baker, H. M.; Norris, G. E.; Rice, D. W.; Baker, E. N. *J. Mol. Biol.* **1989**, *209*, 711.
- (114) Shongwe, M. S.; Smith, C. A.; Ainscough, E. W.; Baker, H. M.; Brodie, A. M.; Baker, E. N. *Biochemistry* **1992**, *31*, 4451.
- (115) Bailey, C. T.; Patch, M. G.; Carrano, C. J. *Biochem.* **1988**, *27*, 6276.
- (116) Baker, E. N.; Lindley, P. F. *J. Inorg. Biochem.* **1992**, *47*, 147.
- (117) Anderson, B. F.; Baker, H. M.; Dodson, E. J. *Proc. Natl. Acad. Sci. U.S.A.* **1987**, *84*, 1769.
- (118) Navati, M. S.; Samuni, U.; Aisen, P.; Friedman, J. M. *Proc. Natl. Acad. Sci. U.S.A.* **2003**, *100*, 3832.
- (119) Patch, M. G.; Carrano, C. J. *Inorg. Chim. Acta* **1981**, *56*, L71.

- (120) Grossmann, J. G.; Neu, M.; Evans, R. W.; Lindley, P. F.; Appel, H.; Hasnain, S. S. *J. Mol. Biol.* **1993**, 229, 585.
- (121) Li, L.; Mu, Q.; Zhang, B.; Yan, B. *Analyst* **2010**, 135, 1519.
- (122) Otsuka, H.; Nagasaki, Y.; Kataoka, K. *Adv. Drug Delivery Rev.* **2003**, 55, 403.
- (123) Niidome, T.; Yamagata, M.; Okamoto, Y.; Akiyama, Y.; Takahashi, H.; Kawano, T.; Katayama, Y.; Niidome, Y. *J. Controlled Release* **2006**, 114, 343.
- (124) Gref, R.; Luck, M.; Quellec, P.; Marchand, M.; Dellacherie, E.; Harnisch, S.; Blunk, T.; Muller, R. H. *Colloids Surf., B* **2000**, 18, 301.
- (125) Aubin-Tam, M. E.; Hamad-Schifferli, K. *Langmuir* **2005**, 21, 12080.
- (126) Chen, B. X.; Wilson, S. R.; Das, M.; Coughlin, D. J.; Erlanger, B. F. *Proc. Natl. Acad. Sci. U.S.A.* **1998**, 95, 10809.
- (127) Delfino, I.; Cannistraro, S. *Biophys. Chem.* **2009**, 139, 1.
- (128) Edri, E.; Regev, O. *Anal. Chem.* **2008**, 80, 4049.
- (129) Jiang, X.; Jiang, J.; Jin, Y.; Wang, E.; Dong, S. *Biomacromolecules* **2005**, 6, 46.
- (130) Kathiravan, A.; Renganathan, R.; Anandan, S. *Polyhedron* **2009**, 28, 157.
- (131) Matsuura, K.; Saito, T.; Okazaki, T.; Ohshima, S.; Yumura, M.; Iijima, S. *Chem. Phys. Lett.* **2006**, 429, 497.
- (132) Nepal, D.; Geckeler, K. E. *Small* **2006**, 2, 406.
- (133) Teichroeb, J. H.; Forrest, J. A.; Jones, L. W. *Eur. Phys. J. E* **2008**, 26, 411.
- (134) Tessier, P. M.; Jinkoji, J.; Cheng, Y. C.; Prentice, J. L.; Lenhoff, A. M. *J. Am. Chem. Soc.* **2008**, 130, 3106.
- (135) Zorbas, V.; Smith, A. L.; Xie, H.; Ortiz-Acevedo, A.; Dalton, A. B.; Dieckmann, G. R.; Draper, R. K.; Baughman, R. H.; Musselman, I. H. *J. Am. Chem. Soc.* **2005**, 127, 12323.
- (136) Casals, E.; Pfaller, T.; Duschl, A.; Oostingh, G. J.; Puentes, V. *ACS Nano* **2010**, 4, 3623.
- (137) Belgorodsky, B.; Fadeev, L.; Ittah, V.; Benyamini, H.; Zelner, S.; Huppert, D.; Kotlyar, A. B.; Gozin, M. *Bioconjugate Chem.* **2005**, 16, 1058.
- (138) Yongli, C.; Xiufang, Z.; Yandao, G.; Nanming, Z.; Tingying, Z.; Xinqi, S. *J. Colloid Interface Sci.* **1999**, 214, 38.
- (139) Fischer, N. O.; Verma, A.; Goodman, C. M.; Simard, J. M.; Rotello, V. M. *J. Am. Chem. Soc.* **2003**, 125, 13387.
- (140) Karlsson, M.; Carlsson, U. *Biophys. J.* **2005**, 88, 3536.
- (141) Lee, I. S.; Lee, N.; Park, J.; Kim, B. H.; Yi, Y. W.; Kim, T.; Kim, T. K.; Lee, I. H.; Paik, S. R.; Hyeon, T. *J. Am. Chem. Soc.* **2006**, 128, 10658.
- (142) Macaroff, P. P.; Oliveira, D. M.; Lacava, Z. G. M.; Azevedo, R. B.; Lima, E. C. D.; Morais, P. C.; Tedesco, A. C. *IEEE Trans. Magn.* **2004**, 40, 3027.
- (143) Mu, Q.; Liu, W.; Xing, Y.; Zhou, H.; Li, Z.; Zhang, Y.; Ji, L.; Wang, F.; Si, Z.; Zhang, B.; Yan, B. *J. Phys. Chem. C* **2008**, 112, 3300.
- (144) Pramanik, S.; Banerjee, P.; Sarkar, A.; Bhattacharya, S. C. *J. Lumin.* **2008**, 128, 1969.
- (145) Sahoo, B.; Goswami, M.; Nag, S.; Maiti, S. *Chem. Phys. Lett.* **2007**, 445, 217.
- (146) Wangoo, N.; Suri, C. R.; Shekhawat, G. *Appl. Phys. Lett.* **2008**, 92, 133104.
- (147) You, C. C.; Miranda, O. R.; Gider, B.; Ghosh, P. S.; Kim, I. B.; Erdogan, B.; Krovi, S. A.; Bunz, U. H. F.; Rotello, V. M. *Nat. Nanotechnol.* **2007**, 2, 318.
- (148) Zhou, H.; Mu, Q.; Gao, N.; Liu, A.; Xing, Y.; Gao, S.; Zhang, Q.; Qu, G.; Chen, Y.; Liu, G.; Zhang, B.; Yan, B. *Nano Lett.* **2008**, 8, 859.
- (149) Pompa, P. P.; Chiuri, R.; Manna, L.; Pellegrino, T.; Del Mercato, L. L.; Parak, W. J.; Calabi, F.; Cingolani, R.; Rinaldi, R. *Chem. Phys. Lett.* **2006**, 417, 351.
- (150) Pons, T.; Medintz, I. L.; Wang, X.; English, D. S.; Mattoussi, H. *J. Am. Chem. Soc.* **2006**, 128, 15324.
- (151) Casanova, D.; Giaume, D.; Moreau, M.; Martin, J. L.; Gacoin, T.; Boilot, J. P.; Alexandrou, A. *J. Am. Chem. Soc.* **2007**, 129, 12592.
- (152) Jiang, X.; Weise, S.; Hafner, M.; Racker, C.; Zhang, F.; Parak, W. J.; Nienhaus, G. U. *J. R. Soc. Interface* **2010**, 7 (Suppl. 1), S5.
- (153) Callender, R.; Deng, H. *Annu. Rev. Biophys. Biomol. Struct.* **1994**, 23, 215.
- (154) Thomas, G. J., Jr. *Annu. Rev. Biophys. Biomol. Struct.* **1999**, 28, 1.
- (155) Karajanagi, S. S.; Vertegel, A. A.; Kane, R. S.; Dordick, J. S. *Langmuir* **2004**, 20, 11594.
- (156) Mandal, H. S.; Kraat, H. B. *J. Am. Chem. Soc.* **2007**, 129, 6356.
- (157) Peng, Z. G.; Hidajat, K.; Uddin, M. S. *J. Colloid Interface Sci.* **2004**, 271, 277.
- (158) Shen, X. C.; Liou, X. Y.; Ye, L. P.; Liang, H.; Wang, Z. Y. *J. Colloid Interface Sci.* **2007**, 311, 400.
- (159) Hong, R.; Fischer, N. O.; Verma, A.; Goodman, C. M.; Emrick, T.; Rotello, V. M. *J. Am. Chem. Soc.* **2004**, 126, 739.
- (160) Srivastava, S.; Verma, A.; Frankamp, B. L.; Rotello, V. M. *Adv. Mater.* **2005**, 17, 617.
- (161) Su, Z.; Leung, T.; Honek, J. F. *J. Phys. Chem. B* **2006**, 110, 23623.
- (162) Verma, A.; Simard, J. M.; Worrall, J. W. E.; Rotello, V. M. *J. Am. Chem. Soc.* **2004**, 126, 13987.
- (163) You, C. C.; De, M.; Han, G.; Rotello, V. M. *J. Am. Chem. Soc.* **2005**, 127, 12873.
- (164) Hellstrand, E.; Lynch, I.; Andersson, A.; Drakenberg, T.; Dahlback, B.; Dawson, K. A.; Linse, S.; Cedervall, T. *FEBS J.* **2009**, 276, 3372.
- (165) Stayton, P. S.; Drobny, G. P.; Shaw, W. J.; Long, J. R.; Gilbert, M. *Crit. Rev. Oral Biol. Med.* **2003**, 14, 370.
- (166) Bhattacharya, J.; Choudhuri, U.; Siwach, O.; Sen, P.; Dasgupta, A. K. *Nanomedicine: NBM* **2006**, 2, 191.
- (167) Inomoto, N.; Osaka, N.; Suzuki, T.; Hasegawa, U.; Ozawa, Y.; Endo, H.; Akiyoshi, K.; Shibayama, M. *Polymer* **2009**, 50, 541.
- (168) Ipe, B. I.; Shukla, A.; Lu, H.; Zou, B.; Rehage, H.; Niemeyer, C. M. *ChemPhysChem* **2006**, 7, 1112.
- (169) You, C. C.; De, M.; Rotello, V. M. *Curr. Opin. Chem. Biol.* **2005**, 9, 639.
- (170) De, M.; You, C. C.; Srivastava, S.; Rotello, V. M. *J. Am. Chem. Soc.* **2007**, 129, 10747.
- (171) Rozhkov, S. P.; Goryunov, A. S.; Sukhanova, G. A.; Borisova, A. G.; Rozhkova, N. N.; Andrievsky, G. V. *Biochem. Biophys. Res. Commun.* **2003**, 303, 562.
- (172) Montes-Burgos, I.; Walczyk, D.; Hole, P.; Smith, J.; Lynch, I.; Dawson, K. A. *J. Nanopart. Res.* **2009**, 12, 47.
- (173) Scapin, G. *Curr. Pharm. Des.* **2006**, 12, 2087.
- (174) Prakasham, R. S.; Devi, G. S.; Rao, C. S.; Sivakumar, V. S.; Sathish, T.; Sarma, P. N. *Appl. Biochem. Biotechnol.* **2010**, 160, 1888.
- (175) Levy, R.; Thanh, N. T. K.; Christopher Doty, R.; Hussain, I.; Nichols, R. J.; Schiffrin, D. J.; Brust, M.; Fernig, D. G. *J. Am. Chem. Soc.* **2004**, 126, 10076.
- (176) Kim, H. R.; Andrieux, K.; Gil, S.; Taverna, M.; Chacun, H.; Desmaele, D.; Taran, F.; Georgin, D.; Couvreur, P. *Biomacromolecules* **2007**, 8, 793.
- (177) Kim, H. R.; Andrieux, K.; Delomenie, C.; Chacun, H.; Appel, M.; Desmale, D.; Taran, F.; Georgin, D.; Couvreur, P.; Taverna, M. *Electrophoresis* **2007**, 28, 2252.
- (178) Dutta, D.; Sundaram, S. K.; Teegarden, J. G.; Riley, B. J.; Fifield, L. S.; Jacobs, J. M.; Addleman, S. R.; Kaysen, G. A.; Moudgil, B. M.; Weber, T. J. *Toxicol. Sci.* **2007**, 100, 303.
- (179) Nagayama, S.; Ogawara, K. i.; Fukuoka, Y.; Higaki, K.; Kimura, T. *Int. J. Pharm.* **2007**, 342, 215.
- (180) Stolnik, S.; Daudali, B.; Arien, A.; Whetstone, J.; Heald, C. R.; Garnett, M. C.; Davis, S. S.; Illum, L. *Biochim. Biophys. Acta, Biomembr.* **2001**, 1514, 261.
- (181) Salvador-Morales, C.; Flahaut, E.; Sim, E.; Sloan, J.; Green, M. L. H.; Sim, R. B. *Mol. Immunol.* **2006**, 43, 193.
- (182) Gessner, A.; Lieske, A.; Paulke, B.; Muller, R. *Eur. J. Pharm. Biopharm.* **2002**, 54, 165.
- (183) Labarre, D.; Vauthier, C.; Chauvierre, C.; Petri, B.; Muller, R.; Chehimi, M. M. *Biomaterials* **2005**, 26, 5075.

- (184) Neuhoﬀ, V.; Arold, N.; Taube, D.; Ehrhardt, W. *Electrophoresis* **1988**, *9*, 255.
- (185) Switzer, R. C., 3rd; Merrill, C. R.; Shifrin, S. *Anal. Biochem.* **1979**, *98*, 231.
- (186) Nishihara, J. C.; Champion, K. M. *Electrophoresis* **2002**, *23*, 2203.
- (187) Unlu, M.; Morgan, M. E.; Minden, J. S. *Electrophoresis* **1997**, *18*, 2071.
- (188) Gessner, A.; Waicz, R.; Lieske, A.; Paulke, B. R.; Mader, K.; Muller, R. H. *Int. J. Pharm.* **2000**, *196*, 245.
- (189) Mu, Q.; Li, Z.; Li, X.; Mishra, S. R.; Zhang, B.; Si, Z.; Yang, L.; Jiang, W.; Yan, B. *J. Phys. Chem. C* **2009**, *113*, 5390.
- (190) Bayraktar, H.; You, C. C.; Rotello, V. M.; Knapp, M. J. *J. Am. Chem. Soc.* **2007**, *129*, 2732.
- (191) Aggarwal, P.; Hall, J. B.; McLeland, C. B.; Dobrovolskaia, M. A.; McNeil, S. E. *Adv. Drug Delivery Rev.* **2009**, *61*, 428.
- (192) Gerdon, A. E.; Wright, D. W.; Cliffl, D. E. *Anal. Chem.* **2005**, *77*, 304.
- (193) Kaufman, E. D.; Belyea, J.; Johnson, M. C.; Nicholson, Z. M.; Ricks, J. L.; Shah, P. K.; Bayless, M.; Pettersson, T.; Feldoto, Z.; Blomberg, E.; Claesson, P.; Franzen, S. *Langmuir* **2007**, *23*, 6053.
- (194) Wittung, P.; Kajanus, J.; Kubista, M.; Malmstrom, B. G. *FEBS Lett.* **1994**, *352*, 37.
- (195) Kudelski, A. *Surf. Sci.* **2009**, *603*, 1328.
- (196) Chang, S. Y.; Zheng, N. Y.; Chen, C. S.; Chen, C. D.; Chen, Y. Y.; Wang, C. R. *J. Am. Soc. Mass Spectrom.* **2007**, *18*, 910.
- (197) Goodman, C. M.; McCusker, C. D.; Yilmaz, T.; Rotello, V. M. *Bioconjugate Chem.* **2004**, *15*, 897.
- (198) Liu, Z. *Nat. Nanotechnol.* **2007**, *2*, 47.
- (199) Xu, C.; Scuseria, G. E. *Phys. Rev. Lett.* **1994**, *72*, 669.
- (200) Kresse, G.; Furthmuller, J. *Comput. Mater. Sci.* **1996**, *6*, 15.
- (201) Bockstedte, M.; Kley, A.; Neugebauer, J.; Scheffler, M. *Comput. Phys. Commun.* **1997**, *107*, 187.
- (202) Ejtehadi, M. R.; Avall, S. P.; Plotkin, S. S. *Proc. Natl. Acad. Sci. U.S.A.* **2004**, *101*, 15088.
- (203) Somorjai, G. A.; Park, J. Y. *Top. Catal.* **2008**, *49*, 126.
- (204) Jain, P.; Pradeep, T. *Biotechnol. Bioeng.* **2005**, *90*, 59.
- (205) Wang, L.; Luo, J.; Schadt, M. J.; Zhong, C. J. *Langmuir* **2010**, *26*, 618.
- (206) Nordgren, C. E.; Tobias, D. J.; Klein, M. L.; Blasie, J. K. *Biophys. J.* **2002**, *83*, 2906.
- (207) Noon, W. H.; Kong, Y.; Jianpeng, M. *Proc. Natl. Acad. Sci. U.S.A.* **2002**, *99*, 6466.
- (208) Braden, B. C.; Goldbaum, F. A.; Chen, B. X.; Kirschner, A. N.; Wilson, S. R.; Erlanger, B. F. *Proc. Natl. Acad. Sci. U.S.A.* **2000**, *97*, 12193.
- (209) Wong-Ekkabut, J.; Baoukina, S.; Triampo, W.; Tang, I. M.; Tieleman, D. P.; Monticelli, L. *Nat. Nanotechnol.* **2008**, *3*, 363.
- (210) Lopez, C. F.; Nielsen, S. O.; Moore, P. B.; Klein, M. L. *Proc. Natl. Acad. Sci. U.S.A.* **2004**, *101*, 4431.
- (211) Srinivas, G.; Klein, M. L. *Nanotechnology* **2004**, *15*, 1289.
- (212) Alizadeh, A.; Parsafar, G. A.; Ejtehadi, M. R. *Int. J. Nanotechnol.* **2009**, *6*, 926.
- (213) Babadi, M.; Everaers, R.; Ejtehadi, M. R. *J. Chem. Phys.* **2006**, *124*, 174708.
- (214) Seyed-Allaei, H.; Ejtehadi, M. R. *Phys. Rev. E: Stat., Nonlinear, Soft Matter Phys.* **2008**, *77*, 031105.
- (215) Quigley, D.; Rodger, P. M. *J. Chem. Phys.* **2008**, *128*, 221101.
- (216) Hooft, R. W. W.; Van Eijck, B. P.; Kroon, J. J. *J. Chem. Phys.* **1992**, *97*, 6690.
- (217) Kawska, A.; Hochrein, O.; Brickmann, J.; Kniep, R.; Zahn, D. *Angew. Chem., Int. Ed.* **2008**, *47*, 4982.
- (218) Reyes-Grajeda, J. P.; Moreno, A.; Romero, A. J. *Biol. Chem.* **2004**, *279*, 40876.
- (219) Lakshminarayanan, R.; Kini, R. M.; Valiyaveetil, S. *Proc. Natl. Acad. Sci. U.S.A.* **2002**, *99*, 5155.
- (220) Freeman, C. L.; Harding, J. H.; Quigley, D.; Rodger, P. M. *Angew. Chem., Int. Ed.* **2010**, *49*, 5135.
- (221) Aubin-Tam, M. E.; Hwang, W.; Hamad-Schifferli, K. *Proc. Natl. Acad. Sci. U.S.A.* **2009**, *106*, 4095.
- (222) Bauernschmitt, R.; Ahlrichs, R.; Hennrich, F. H.; Kappes, M. M. *J. Am. Chem. Soc.* **1998**, *120*, 5052.
- (223) Gao, H.; Kong, Y. *Annu. Rev. Mater. Res.* **2004**, *34*, 123.
- (224) Shukla, M. K.; Dubey, M.; Zakar, E.; Namburu, R.; Leszczynski, J. *Chem. Phys. Lett.* **2010**, *496*, 128.
- (225) Harris, N. C.; Kiang, C. H. *Phys. Rev. Lett.* **2005**, *95*, 1.
- (226) Milam, V. T.; Hiddessen, A. L.; Crocker, J. C.; Graves, D. J.; Hammer, D. A. *Langmuir* **2003**, *19*, 10317.
- (227) Park, S. Y.; Lytton-Jean, A. K. R.; Lee, B.; Weigand, S.; Schatz, G. C.; Mirkin, C. A. *Nature* **2008**, *451*, 553.
- (228) Hsu, C. W.; Sciortino, F.; Starr, F. W. *Phys. Rev. Lett.* **2010**, *105*, 055502.
- (229) Chia, W. H.; Largo, J.; Sciortino, F.; Starr, F. W. *Proc. Natl. Acad. Sci. U.S.A.* **2008**, *105*, 13711.
- (230) Chithrani, B. D.; Ghazani, A. A.; Chan, W. C. W. *Nano Lett.* **2006**, *6*, 662.
- (231) Noguchi, H.; Takasu, M. *Biophys. J.* **2002**, *83*, 299.
- (232) Choe, S.; Chang, R.; Jeon, J.; Viola, A. *Biophys. J.* **2008**, *95*, 4102.
- (233) Anderson, J. M. *Annu. Rev. Mater. Res.* **2001**, *31*, 81.
- (234) Hubbell, J. A. *Nat. Biotechnol.* **1995**, *13*, 565.
- (235) Mossman, B. T.; Churg, A. *Am. J. Respir. Crit. Care Med.* **1998**, *157*, 1666.
- (236) Donaldson, K.; Stone, V.; Gilmour, P. S.; Brown, D. M.; Macnee, W. *Philos. Trans. R. Soc. London, A* **2000**, *358*, 2741.
- (237) Sayes, C. M.; Fortner, J. D.; Guo, W.; Lyon, D.; Boyd, A. M.; Ausman, K. D.; Tao, Y. J.; Sitharaman, B.; Wilson, L. J.; Hughes, J. B.; West, J. L.; Colvin, V. L. *Nano Lett.* **2004**, *4*, 1881.
- (238) Baugh, J. A.; Donnelly, S. C. *J. Endocrinol.* **2003**, *179*, 15.
- (239) Maderna, P.; Godson, C. *Biochim. Biophys. Acta* **2003**, *1639*, 141.
- (240) Carter, J. M.; Corson, N.; Driscoll, K. E.; Elder, A.; Finkelstein, J. N.; Harkema, J. N.; Gelein, R.; Wade-Mercer, P.; Nguyen, K.; Oberdorster, G. *J. Occup. Environ. Med.* **2006**, *48*, 1265.
- (241) Olmedo, D. G.; Tasat, D. R.; Guglielmotti, M. B.; Cabrini, R. L. *J. Biomed. Mater. Res., Part A* **2005**, *73*, 142.
- (242) Booth, D. R.; Sunde, M.; Bellotti, V.; Robinson, C. V.; Hutchinson, W. L.; Fraser, P. E.; Hawkins, P. N.; Dobson, C. M.; Radford, S. E.; Blake, C. C. F.; Pepys, M. B. *Nature* **1997**, *385*, 787.
- (243) Kreuter, J.; Shamenkov, D.; Petrov, V.; Ramge, P.; Cychutek, K.; Koch-Brandt, C.; Alyautdin, R. *J. Drug Targeting* **2002**, *10*, 317.
- (244) Veiseh, M.; Gabikian, P.; Bahrami, S. B.; Veiseh, O.; Zhang, M.; Hackman, R. C.; Ravanpay, A. C.; Stroud, M. R.; Kusuma, Y.; Hansen, S. J.; Kwok, D.; Munoz, N. M.; Sze, R. W.; Grady, W. M.; Greenberg, N. M.; Ellenbogen, R. G.; Olson, J. M. *Cancer Res.* **2007**, *67*, 6882.
- (245) Minchin, R. F.; Martin, D. J. *Endocrinology* **2010**, *151*, 474.
- (246) Nel, A.; Xia, T.; Mädler, L.; Li, N. *Science* **2006**, *311*, 622.
- (247) Ozin, G. A.; Cademartiri, L. *Small* **2009**, *5*, 1240.
- (248) Fadeel, B.; Garcia-Bennett, A. E. *Adv. Drug Delivery Rev.* **2010**, *62*, 362.